RSC Advances

PAPER

View Article Online
View Journal | View Issue

Cite this: *RSC Adv.*, 2025, **15**, 23146

Heat transfer fluids: amino acid anion ionic liquid based IoNanofluids with remarkable thermal conductivity and low viscosity†

Anshu Chandra,[a] Yamini Sudha Sistla,*[a] Mir Atiq Ahmed,[a] Durga Vijay Shankar Vasireddy,[a] Nancy Jaglan,[b] Nipu Kumar Das,[c] Tamal Banerjee[c] and Venkata Subbarayudu Sistla[d]

Present study aims to develop ionic liquid based nanofluids (IoNanofluids) exhibiting low viscosity, high thermal conductivity, thermal stability, high specific heat capacity and colloidal stability for potential heat transfer fluids applications. Four amino acid anion ionic liquids (AAIL) such as 1-butyl,3-metylimidazolium glycinate, 1-butyl,3-metylimidazolium arginate, 1-ethyl,3-metylimidazolium glycinate, 1-ethyl,3-metylimidazolium arginate were synthesized. The IoNanofluids (INF) were developed by adding 0.05 wt% of MWCNT to the AAILs. The effect of MWCNT concentration and surfactant was investigated by developing INFs consisting of 1-butyl, 3-methylimidazolium tetrafluoroborate ($[bmim]^+[BF_4]^-$) and MWCNT in the range of 0.025–0.1 wt%. The AAILs showed significantly less viscosity (18–8 mPa s at 298 K), higher thermal conductivity and specific heat capacity compared to several conventional ionic liquids. The four AAIL INFs showed 21–40% enhancement in thermal conductivity; very less viscosity (20 mPa s *vs.* 110 mPa s at 300 K), and remarkably higher specific heat capacity (10 J g^{-1} °C *vs.* 1 J g^{-1} °C) compared to $[bmim]^+[BF_4]^-$ INF. The AAIL INFs showed fine and homogeneous dispersion of MWCNT and substantially higher colloidal stability (30 days) compared to $[bmim]^+[BF_4]^-$ (7 days) and $[bmim]^+[BF_4]^-$ + MWCNT + CTAB (14 days). The AAIL INFs of present study showed enhanced heat transfer properties than several literature reported INFs made from conventional ionic liquids. Therefore, based on the overall properties, the AAIL INFs developed in present study could be suitable for applications such as heat exchangers, thermal energy storage systems, cooling of microprocessor systems broadly in the temperature range of 0–200 °C.

Received 28th May 2025
Accepted 30th June 2025

DOI: 10.1039/d5ra03752b

rsc.li/rsc-advances

1. Introduction

Heat transfer fluids (HTFs) are essential in various industrial processes to facilitate the efficient transfer, distribution, and storage of thermal energy. Their primary function is to regulate the temperature by either absorbing or dissipating the heat within a system, ensuring process stability and operational efficiency.[1–3] HTFs are widely utilized across multiple industries, including oil and gas, polymer processing, aerospace, marine engineering, wood processing, biofuel production, food processing, and solar energy systems. In these applications, HTFs provide precise temperature control, uniform heat distribution, and operational reliability. A potential heat transfer fluid should possess properties such as high thermal stability, low freezing point, high thermal conductivity, low viscosity, low vapor pressure and high volumetric heat capacity while being non-toxic, environmentally friendly, non-corrosive and low cost. HTFs can be broadly categorized based on their composition and temperature range.[1–3] Water is the most used HTF due to its high specific heat capacity, cost-effectiveness, and ease of handling. However, due to limited operational temperature range, dictated by freezing at 273.15 K and boiling at 373.15 K under standard atmospheric conditions, its applicability as HTF is restricted for very few applications only. Organic-based HTFs such as ethylene glycol and aromatic compounds exhibit low vapor pressures and high thermal stability but suffer from oxidation at elevated temperatures, reducing their lifespan.[3–5] Silicone-based HTFs, though more oxidation-resistant, typically have low thermal conductivities.[4] HTFs are further classified into three categories based on their operational temperature range: low-temperature (operating temperatures up to 273 K) such as glycols, medium-temperature (operating temperatures up to 593 K) such as silicone oil and certain salts, and high-temperature (operating temperatures

[a]*Department of Chemical Engineering, Shiv Nadar Institution of Eminence, Delhi-NCR, India. E-mail: yamini.sistla@snu.edu.in*
[b]*Department of Physics, Shiv Nadar Institution of Eminence, Delhi-NCR, India*
[c]*Department of Chemical Engineering, Indian Institute of Technology Guwahati, India*
[d]*Rajiv Gandhi Institute of Petroleum Technology, Raebareli, India*

† Electronic supplementary information (ESI) available. See DOI: https://doi.org/10.1039/d5ra03752b

above 593 K) such as molten salts.[4–6] Most of the commercially available HTFs operate within the low-to-medium temperature range, only a limited selection of specialized fluids can withstand high-temperature applications.[7] Researchers Choi and Eastman were reportedly the first to introduce the term nanofluids.[8] Nanofluids are typically developed by adding nanoparticles (10–100 nm) to the solvents to improve the thermal conductivity of the resulting nanofluids, as the nanoparticles will improve heat conduction.[9,10] Deep eutectic solvents (DES) were also used as base fluids for developing nanofluids for heat transfer applications.[11–13] Researchers have developed nanofluids consisting of ammonium and phosphonium based DES along with graphene, Al_2O_3 nanoparticles.[11–13]

A promising alternative for low and medium temperature HTFs are ionic liquids (ILs).[14,15] ILs are defined as salts composed of organic cation and organic/inorganic anion having melting points usually below 373.15 K.[15] ILs exhibit several unique properties such as negligible saturated vapor pressure, high thermal stability, non-flammable nature, oxidation resistance, high heat capacity, a wide liquidity range, due to the presence of coulombic interactions between the cation and anion, hydrogen bonding and van der Waals interactions. Additionally, their inherent recyclability, non-toxicity, and tunable properties make them attractive candidates for several applications including HTFs.[14–17] Industrial processes operating at extreme temperatures, ranging from cryogenic conditions (as low as 158 K) to elevated temperatures (up to 593 K), require HTFs with broad range of thermal stability.[18] The wide liquid-phase range of ILs present a viable solution to this challenge. Further enhancements in HTF performance have been achieved through the incorporation of nanoparticles into ILs, resulting in the formation of IoNanofluids (INF).[16–18] Nanoparticles such as boron nitride, single walled carbon nanotubes (SWCNT), multi walled carbon nanotubes (MWCNT), graphene, graphite flakes, activated carbon and mesoporous carbon were typically used to produce nanofluids.[18] The nanoparticles act as thermal bridges which generate favourable paths for heat transfer. The dispersion of nanoparticles in ILs improves the thermal conductivity, heat capacity, and overall thermophysical performance.[16–19] Thus, IL based nanofluids (IoNanofluids, INF) have garnered significant research interest as potential HTFs, particularly in low and medium temperature systems where conventional HTFs exhibit performance limitations. Researchers have developed INFs based on cations such as 1-alkyl, 3-methylimidazolium, pyrrolidinum, ammonium and phosphonium and anions such as $[BF_4]^-$, $[PF_6]^-$, $[TF_2N]^-$, $[CF_3SO_3]^-$, $[(CF_3SO_2)_2N]^-$, $[DCA]^-$, $[EtSO_4]^-$, and $[CH_3SO_3]^-$ to name a few.[16–19]

For any HTF, thermal conductivity and viscosity are the most critical parameters along with density and specific heat capacity. Oster *et al.*[20] have developed INFs from trihexyl(tetradecyl)phosphonium ($[P_{14,6,6,6}]^+$) cation along with anions such as acetate, butanoate, hexanoate, octanoate or decanoate. They developed nanofluids by adding carbon nanotubes, boron nitride, graphite or mesoporous carbon as nanoparticles with concentration up to 3 wt% and analysed the HTFs for various properties.[20] They reported that the carbon nanotube based INFs exhibited highest thermal conductivity followed by boron nitride, graphite and mesoporous carbon. The highest thermal conductivity in their studies was exhibited by $[P_{14,6,6,6}]^+$[acetate]$^-$ (0.1602 W m^{-1} K^{-1} at 298 K) and the lowest was exhibited by $[P_{14,6,6,6}]^+$[hexanoate]$^-$ (0.156 W m^{-1} K^{-1} at 298 K).[20] The viscosity of the INFs was in the range of 20–110 mPa s based on the type of nanoparticle and weight fraction of nanoparticle.[20] Jozwiak *et al.*[21] have reported SWCNT and MWCNT incorporated $[emim]^+[SCN]^-$ based HTFs. They reported that the thermal conductivity of 1 wt% SWCNT incorporated $[emim]^+[SCN]^-$ was 0.3 W m^{-1} K^{-1}. The viscosity of the INFs developed by Jozwiak *et al.* was in the range of 100–300 mPa s.[21] Nieto de Castro *et al.*[22] have developed $[emim]^+[DCA]^-$ nanofluid by adding 0.5 wt% titanium oxide nanoparticles. The thermal conductivity and viscosity of the nanofluid at 298 K were 0.201 W m^{-1} K^{-1} and 17 mPa s respectively. Franca *et al.*[23] have developed $[emim]^+[SCN]^-$, $[emim]^+$[Tricyanide]$^-$ based nanofluids by adding 0.5 wt% and 1 wt% MWCNT. They reported thermal conductivity of 0.19 W m^{-1} K^{-1} for 0.5 wt% MWCNT added $[emim]^+[SCN]^-$.[23] Zhang *et al.*[24] have studied $[emim]^+$[Acetate]$^-$ IL by adding graphene nanoparticle. The nanofluid showed the thermal conductivity of 0.25 W m^{-1} K^{-1} and viscosity of 100 mPa s at 300 K.[24] Stoppa *et al.*[25] have studied the effect of alkyl chain length on the electrical conductivity of some imidazolium cation and $[BF_4]^-$ anion ionic liquids in a wide temperature range of −35–195 °C. Liang *et al.*[26] have synthesized ILs 1-ethyl-4-alkyl-1,2,4-triazolium alanine [Taz(2,-*n*)]$^+$[Ala]$^-$, (n = 4, 5) and reported the surface tension, isobaric molar heat capacity, and thermal conductivity. The synthesized triazole based ILs showed heat storage density of ∼2.63 MJ m^{-3} K^{-1}, thermal conductivity of ∼0.190 W m^{-1} K^{-1}, and melting temperature of ∼226 K.[26] Some of the commercial HTFs such as Dowtherm A, Dowtherm G, Dowtherm J, Dowtherm MX, Dowtherm Q, Dowtherm RP, Dowtherm T, Syltherm XLT, Syltherm 800, and Syltherm HF have thermal conductivity values of 0.139, 0.126, 0.128, 0.123, 0.122, 0.131, 0.130, 0.11, 0.135 and 0.107 W m^{-1} K^{-1} respectively and the viscosities of 4.29, 12.5, 0.91, 20.3, 4.0, 42.82, 30.55, 1.4, 10.03 and 1.84 mPa s respectively at 293 K.[26]

Though some of the IL based nanofluids have displayed encouraging properties suitable for HTF applications, factors such as high synthesis costs, relatively high viscosity becomes challenging. On the other hand, the low viscosity INFs reported in the literature suffer from low thermal conductivity. In this regard, the focus of the present study was to investigate the potential of amino acid anion ionic liquid (AAIL) based IoNanofluids (AAIL INF) as cost effective next generation HTFs. Further, the AAILs would show better biodegradability and biocompatibility as they do not consist of any halogen atoms and only have amine and carboxylic groups.[27–29] Based on our previous work, AAILs offer low synthesis costs due to the low cost of the amino acid compounds and less complicated synthesis procedure.[27] The present study discusses the synthesis of AAILs and the AAIL INFs obtained by incorporating multi-walled carbon nanotubes (MWCNT) as nanoparticle additives in various concentrations. The MWCNTs are known for their low cost, higher availability, high thermal conductivity,

high aspect ratio, large surface area and more stability of nanoparticle dispersion which would enhance the thermal conductivity and heat transfer efficiency of nanofluids compared to other nanoparticles such as SWCNT, graphene, metal oxides and carbon quantum dots.[30] The investigated AAILs include 1-butyl-3-methylimidazolium glycinate ($[bmim]^+[Gly]^-$), 1-butyl-3-methylimidazolium arginate ($[bmim]^+[Arg]^-$), 1-ethyl-3-methylimidazolium glycinate ($[emim]^+[Gly]^-$), and 1-ethyl-3-methylimidazolium arginate ($[emim]^+[Arg]^-$). For comparison purpose and to study the effect of MWCNT concentration and the effect of surfactant on the nanoparticle dispersion, thermal conductivity and colloidal stability, a commercially available IL 1-butyl-3-methylimidazolium tetrafluoroborate ($[bmim]^+[BF_4]^-$) was used.

2. Experimental details

2.1. Materials

S. No	Chemical name	CAS number	Purity	Company
1	1-Butyl,3-methylimidazolium tetrafluoroborate ($[bmim]^+[BF_4]^-$)	174501-65-6	≥98%	Sigma Aldrich
2	1-Butyl,3-methylimidazolium bromide ($[bmim]^+[Br]^-$)	85100-77-2	≥97%	Sigma Aldrich
3	1-Ethyl,3-methylimidazolium bromide ($[emim]^+[Br]^-$)	65039-08-9	≥97%	Sigma Aldrich
4	Glycine	56-40-6	≥98.5%	Sigma Aldrich
5	L-Arginine	74-79-3	≥98%	Sigma Aldrich
6	AmberLite™ IRN-78 (OH^- resin)	11128-95-3		Thermo Fisher Scientific
7	Tween 80	9005-65-6	≥99%	Sigma Aldrich
8	Lecithin/L-α-phosphatidylcholine (from soybean)	8002-43-5	≥99%	Sigma Aldrich
9	Cetyltrimethylammonium bromide (CTAB)	57-09-0	≥98%	Sigma Aldrich
10	Sodium dodecyl sulphate (SDS)	151-21-3	≥99%	Sigma Aldrich
11	Multiwalled carbon nanotubes (MWCNT)	308068-56-6	≥95%	Sigma Aldrich

2.2. Synthesis of amino acid anion ionic liquid

A brief description of the synthesis procedure of the investigated amino acid anion ionic liquids is as follows.[27] Initially, 25 g of $[bmim]^+[Br]^-$ was dissolved in 50 ml of double distilled water. The aqueous solution of $[bmim]^+[Br]^-$, with an equimolar amount of OH^- resin IRN-78 added was kept under stirring using a magnetic stirrer at 350 rpm for 48 h at room temperature and pressure. The obtained aqueous solution of $[bmim]^+[OH]^-$ was then added to the aqueous solution of 20% excess amino acid and stirred using a magnetic stirrer for 24 h. The water was then evaporated in a rotary evaporator. The resulting solution was washed with acetonitrile and ethanol mixture to get the desired ionic liquid and precipitate out the unreacted amino acid. After separating the precipitate with filtration, solvent was evaporated using rotary evaporator for 4 h to remove any traces of solvent. The AAILs were obtained with 80–85% yield on the basis of the cation precursor IL taken. Four amino acid anion ILs were synthesized by using the above procedure: 1-butyl,3-methylpyrrolidinium Glycinate ($[bmim]^+[Gly]^-$), 1-butyl,3-methylpyrrolidinium Arginate ($[bmim]^+[Arg]^-$), 1-ethyl,3-methylpyrrolidinium Glycinate ($[emim]^+[Gly]^-$), 1-ethyl,3-methylpyrrolidinium Arginate ($[emim]^+[Arg]^-$). The molecular structures of the cations and anions are given in Table 1.

Table 1 Molecular structures of AAILs

Ion	Structure
$[emim]^+$	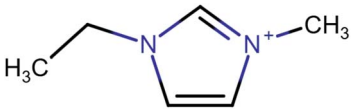
$[bmim]^+$	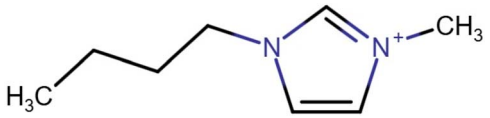
$[Gly]^-$	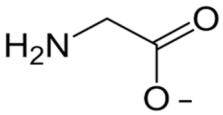
$[Arg]^-$	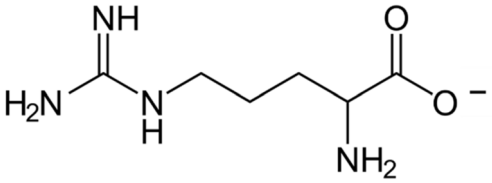

2.3. Preparation of IoNanofluids (INFs)

The INFs were prepared by adding desired weight percent of MWCNT to the IL under magnetic stirring for 1 h at 1400 rpm. The details of the composition of INFs synthesized are reported in Table 2 and 3. The INF was then homogenized using ultrasonic homogenizer for breaking any nanoparticle agglomerations and to get fine and uniform distribution/homogenization. To study the effect of MWCNT concentration, $[bmim]^+[BF_4]^-$ based INFs were prepared by adding 0.025, 0.05, 0.075 and 0.1 wt% of MWCNT. To improve the uniform and fine dispersion of MWCNT and colloidal stability, surfactant was added in equal concentration of MWCNT to the INF. To evaluate the surfactant effect on INF properties, the INF having 0.05 wt% MWCNT was chosen. The most suitable surfactant was identified by adding surfactants such as CTAB, SDS, Tween 80 and lecithin in 0.05 wt% concentration to the INF. The most suitable surfactant was chosen based on the size of nanoparticle agglomerations, uniformity in the dispersion of nanoparticles and colloidal stability of the INF.

Table 2 Composition of $[bmim]^+[BF_4]^-$ based IoNanofluids

Code	Mass of $[bmim][BF_4]$ (g)	Mass of MWCNT (g)	% wt MWCNT	Surfactant used	Mass of surfactant (g)	Density (g cm^{-3})
ILCNT1	14.00	0.0037	0.025	—	—	1.212
ILCNT2	14.00	0.0072	0.050	—	—	1.215
ILCNT3	14.00	0.0108	0.075	—	—	1.218
ILCNT4	14.00	0.0144	0.100	—	—	1.223
ILCNT5	14.00	0.0036	0.025	CTAB	0.004	1.212
ILCNT6	14.00	0.0071	0.050	CTAB	0.007	1.215
ILCNT6T	6.00	0.0030	0.050	Tween 80	0.003	1.215
ILCNT6L	6.00	0.0030	0.050	Lecithin	0.003	1.215
ILCNT6S	6.00	0.0033	0.050	SDS	0.003	1.215
ILCNT7	14.00	0.0108	0.075	CTAB	0.011	1.217
ILCNT8	14.00	0.0140	0.100	CTAB	0.014	1.221

Table 3 Composition of amino acid-anion based IoNanofluids

Code	Ionic liquid used	Mass of IL (g)	Mass of MWCNT (g)	% wt MWCNT	Mass of CTAB (g)	Density (g cm^{-3})
BGCNT2	$[bmim]^+[Gly]^-$	7.00	0.0035	0.05	—	1.19
BACNT6	$[bmim]^+[Arg]^-$	7.00	0.0036	0.05	0.0037	1.18
EGCNT6	$[emim]^+[Gly]^-$	7.00	0.0035	0.05	0.0036	1.25
EACNT2	$[emim]^+[Arg]^-$	7.00	0.0035	0.05	—	1.23

The AAIL INFs were prepared by adding 0.05 wt% of MWCNT. For the AAIL INFs, 0.05 wt% of CTAB was added to investigate the improvement in the uniform dispersion of MWCNT and colloidal stability. The list of $[bmim]^+[BF_4]^-$ based and AAIL based INFs studied in the present work and their codes are mentioned in the Tables 2 and 3 respectively. As the studies on $[bmim]^+[BF_4]^-$ + MWCNT INFs confirmed that CTAB is promising surfactant, only CTAB was chosen as surfactant for AAIL INFs.

2.4. Characterization

2.4.1. Fourier transform infrared spectroscopy (FTIR). FTIR was used to confirm the successful synthesis of AAILs. The spectrum was obtained within the 400–4000 cm^{-1} range with a resolution of 4 cm^{-1} using Thermo Fisher Nicolet iS20 FTIR Spectrometer.

2.4.2. Density. Density measurements are important for HTFs to get an idea about the pumping energy required to transport the fluid. For example, if the HTF is highly dense, it would require high pumping energy for the fluid transport. The density of the AAIL and INFs was measured by weighing the mass of 1 ml of the sample in a high precision Mettler Toledo Microbalance. This procedure was repeated five times to account for any measurement errors. The final density measurement was taken as the average of the five readings.

2.4.3. Viscosity. Viscosity is one of the most crucial parameters for HTFs, which is related to the fluidity and ease of transportation of the fluid. A stress controlled Modular Compact Rheometer (MCR302, Anton Paar, USA) was used to perform the rheology studies. HTFs are often utilised in applications which work at high temperatures. Analysing viscosity at elevated temperatures is important as it shows if there is a significant change in viscosity at high temperatures. Therefore, change in viscosity was studied against increasing temperature in the range of 10–100 °C. Analysing viscosity against increasing shear rate tells us how the fluid would behave in different flow conditions. It also talks about the Newtonian or non-Newtonian behaviour of the fluid. Therefore, viscosity was evaluated against increasing shear rate in the range of 0.1–1000 s^{-1}.

2.4.4. Thermogravimetric Analysis (TGA). Thermogravimetric Analysis (TGA) was used to study the decomposition of the studied INFs when subjected to heat. The TGA was done using Mettler Toledo Small Furnace TGA2 with a heating rate of 10 °C min^{-1} in the temperature range of 30–600 °C. The thermal stability of the INFs as studied from TGA analysis is very important to comprehend the efficient operating temperature range of the INFs and therefore the targeted applications. Further, the TGA also elucidates the effect of the composition (nanoparticles, base fluid, surfactant, stabilizer, moisture presence during base fluid synthesis *etc.*) on the degradation phenomena/thermal stability/oxidation stability of the INF.

2.4.5. Differential scanning calorimetry (DSC). Differential Scanning Calorimetry (DSC) is a technique used to measure the heat flow in and out of the sample as a function of temperature to comprehend the thermal transitions in the sample. Understanding the thermal behaviour in terms of phase transition temperature, specific heat capacity, degradation temperature of IL (base fluid) and INFs is crucial for assessing their overall performance as HTFs under operating conditions of a particular application. For instance, specific heat capacity (amount of heat

required to raise the temperature of a unit mass of sample by unit degree Celsius) is related to the amount of heat energy that can be absorbed, stored and transferred by the INF. Further, the crystallization, melting and degradation temperatures identified from DSC would help in identifying the operating temperature range for a INF. The DSC analysis was done using TA thermal instrument's DSC 2500. Since all the samples are in liquid phase, to evaluate the prospective operating temperature range and to capture the glass transition temperature as well, the DSC analysis was done from the lowest temperature possible for the instrument used *i.e.* −80 °C to 310 °C with a heating rate of 10 °C min^{-1}.

2.4.6. Thermal conductivity. Thermal conductivity, defined as the ability of the fluid to conduct heat, is the most important parameter for a heat transfer fluid. The thermal conductivity of the AAILs and INFs developed in the present study was measured using KD2 Pro Thermal Properties Analyzer (Decagon, USA). This instrument works on the Transient Hot Wire (THW) method. The analyser is equipped with 100 mm length single-needle TR-1 type sensor having needle diameter of 2.4 mm. The thermal conductivity range of the instrument is 0.1–4.00 W m^{-1} K^{-1} having an accuracy of ± 10% for the measurements in the range of 0.2–4 W m^{-1} K^{-1} and ±0.02 W m^{-1} K^{-1} for the measurements in the range of 0.1–0.2 W m^{-1} K^{-1}. The analyser was calibrated with standard glycerine. All the measurements were performed at 302 ± 1.19 K. For pure $[bmim]^+[BF_4]^-$ and $[bmim]^+[Arg]^-$ + MWCNT, thermal conductivity was also measured in the temperature range of 25–54 °C. To avoid any natural convection and to make sure that the heat transfer happens through conduction only, the measuring sample was placed in a small diameter tube.

2.4.7. Microscopic analysis. The size of agglomerations and uniformity of dispersion of MWCNT and the effect of surfactant in the studied HTFs was analysed through microscopic analysis. Olympus inverted microscope CKX-53 was used at a scale of 100 μm.

2.4.8. Colloidal stability. Another crucial performance indicator for HTFs is the colloidal stability. The colloidal stability of the studied HTFs was visually analysed by keeping the sample vials undisturbed and the colloidal separation was checked every day multiple times by using a backlight. The visual observation method was used as this is simple, inexpensive and provides quick qualitative visual impression and information about the nanoparticle sedimentation in the nanofluid at macroscopic level over time.

3. Results and discussion

3.1. Characterization of MWCNT

The morphology of the procured MWCNT was studied using JSM-7610F Plus Field Emission Scanning Electron Microscopy (FESEM). The FESEM images as presented in Fig. 1(a) and (b) show that the MWCNT had interwoven bundles with uniform microstructure. The outer diameter of the nanotube was in the range of 37–53 nm. The FTIR of MWCNT is presented in Fig. 1(c). The FTIR of the MWCNT displays only two peaks at ~3450 cm^{-1} and ~1550 cm^{-1}. No other distinctive peaks corresponding to any functional groups were present. The peak at ~3450 cm^{-1} corresponds to O–H stretch which might be present as impurity from synthesis and the other peak at ~1550 cm^{-1} corresponds to C=C stretching of MWCNT. This confirms that the procured MWCNT was pure carbon without any modification/functionalization.

3.2. Characterization of amino acid anion ionic liquids (AAIL)

The molecular structures of the cations and anions of the four AAILs synthesized are presented in Table 1. The four AAILs were characterized by FTIR to make sure of successful synthesis by analysing the functional groups present as shown in the Fig. 2. Fig. 2(a) compares the FTIR of the synthesized $[bmim]^+[Gly]^-$ with the cation and anion precursors $[bmim]^+[Br]^-$ and glycine respectively. Fig. 2(b) presents the FTIR of the other three AAILs $[bmim]^+[Arg]^-$, $[emim]^+[Gly]^-$, and $[emim]^+[Arg]^-$. For all the four AAILs, the presence of –COO group stretch was confirmed from the characteristic FTIR peaks at ~1400, 1580, 1630 cm^{-1} while the sharp peak at ~3300 cm^{-1} corresponds to N–H stretch of $–NH_2$.

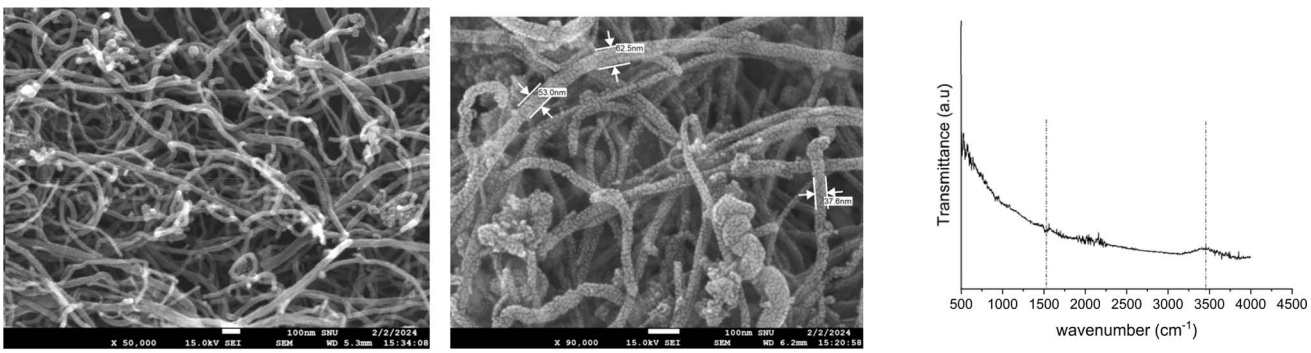

Fig. 1 MWCNT characterization (a) and (b) FESEM (c) FTIR.

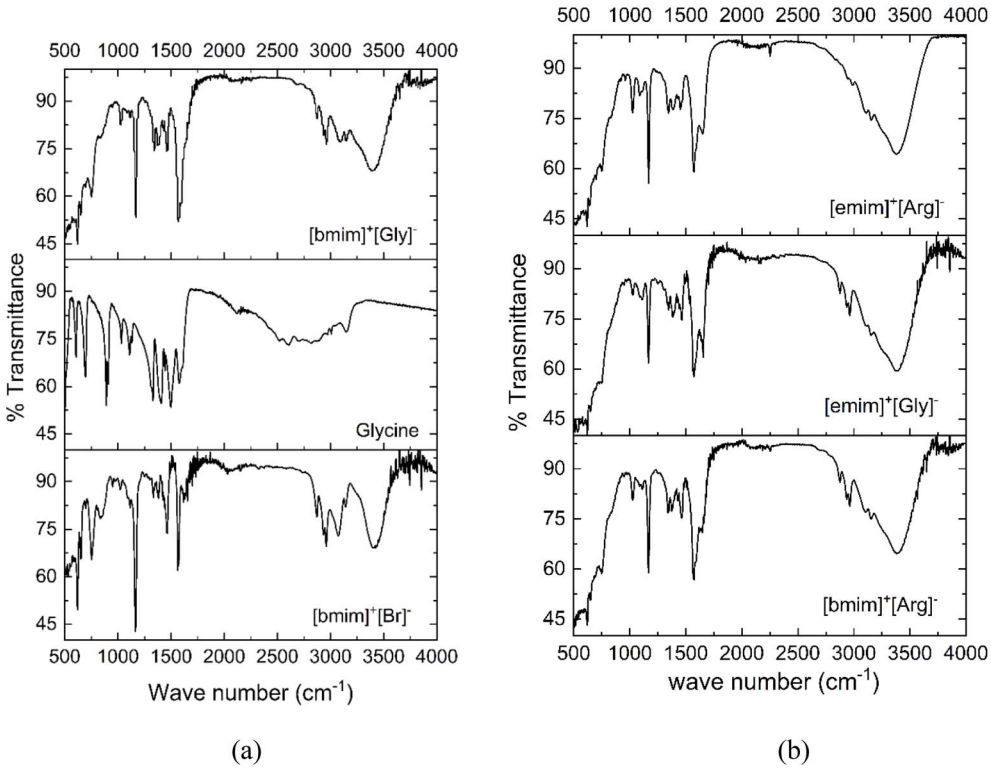

Fig. 2 (a) FTIR of synthesized $[bmim]^+[Gly]^-$ with reference to the starting materials $[bmim]^+[Br]^-$ and Glycine (b) FTIR of $[emim]^+[Gly]^-$, $[emim]^+[Arg]^-$, $[bmim]^+[Arg]^-$.

The density of $[bmim]^+[Gly]^-$, $[bmim]^+[Arg]^-$, $[emim]^+[Gly]^-$, and $[emim]^+[Arg]^-$ as per the procedure mentioned in the methodology section was found out to be 1.14, 1.13, 1.19 and 1.09 g cm^{-3} respectively. The density of the AAILs was observed to be less than several conventional non-amino acid anion ionic liquids. For example, densities of conventional 1-butyl-3-methylimidazolium bis(trifluoromethylsulfonyl) ($[bmim]^+[TF_2N]^-$) and $[bmim]^+[BF_4]^-$ are 1.44 g cm^{-3} and 1.21 g cm^{-3} respectively[31,32] which are higher than the AAILs synthesized in the present work.

The prospective heat transfer fluids should have low viscosity for easy flow in the pipelines, efficient heat transfer while overcoming mass transfer limitations, less pressure drop and low pumping costs. The viscosity of the synthesized AAILs were compared with that of procured commercial IL $[bmim]^+[BF_4]^-$ and presented in Fig. 3. The Fig. 3 clearly illustrates that the

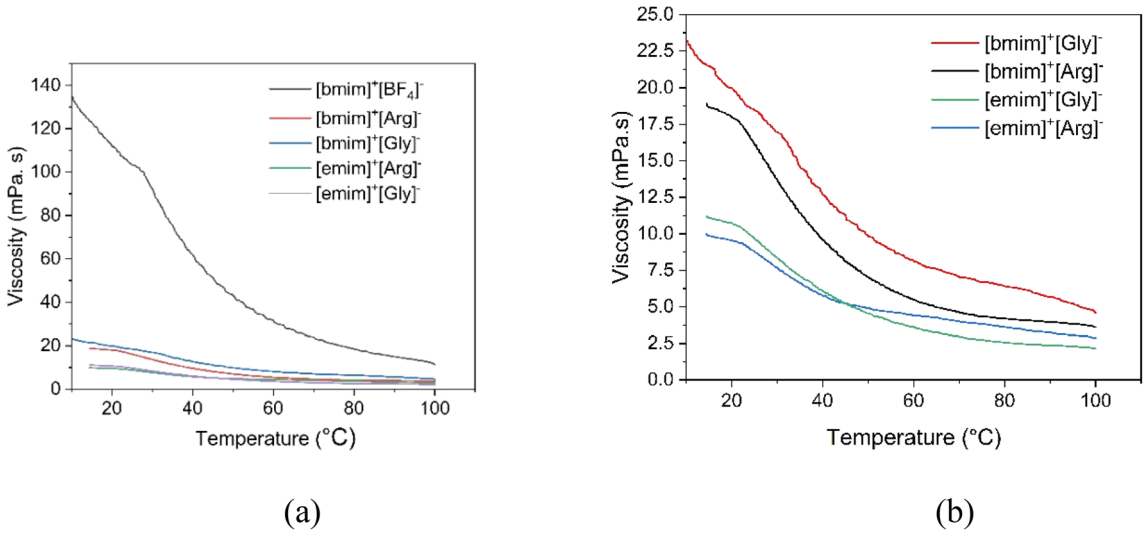

Fig. 3 Comparison of viscosity of synthesized AAILs with commercial $[bmim]^+[BF_4]^-$ in the temperature range of 10–100 °C.

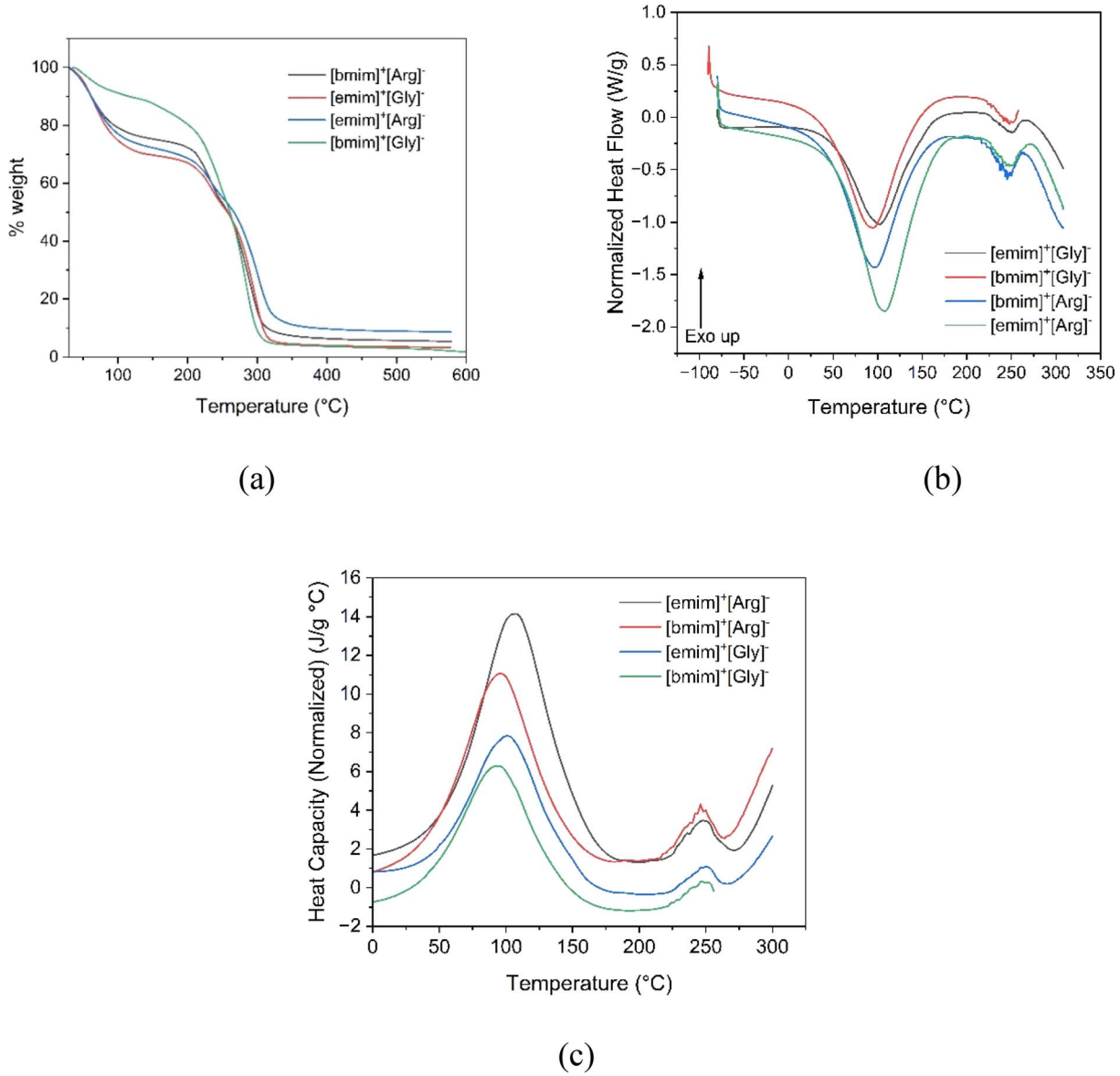

Fig. 4 (a) Thermo gravimetric analysis and (b) heat flow *vs.* temperature (c) heat capacity *vs.* temperature of AAILs.

synthesized AAILs had substantially low viscosity compared to commercial $[bmim]^+[BF_4]^-$. For instance, at 10 °C, the viscosity of $[bmim]^+[BF_4]^-$ was 130 mPa s while that of synthesized AAILs ranged between 10–22.5 mPa s. Therefore, it can be confirmed that the synthesized AAILs exhibited significantly less viscosity. Further, for a particular amino acid anion, the viscosity of $[emim]^+$ cation AAIL showed less viscosity than the one with $[bmim]^+$ cation. This is because of the shorter alkyl chain of $[emim]^+$ which offers more ion mobility and weak intermolecular interactions compared to its longer alkyl chain counterpart $[bmim]^+$. Also, for a fixed cation, glycinate anion showed higher viscosity compared to argininate anion. The smaller molecular structure of glycinate results in less charge delocalization. This leads to stronger interionic interaction with the cation. Therefore, glycinate forms more structured network with cation which hinders free movement of ions of AAIL molecules. On contrary, argininate is a large molecule which therefore results in more charge delocalization. Therefore, argininate will have less interionic interactions with cation which therefore allows relatively more free movement of ions of AAIL molecules. Furthermore, the effect of temperature on viscosity was evaluated in the range of 10–100 °C. With increase in temperature, the viscosity of AAILs got reduced further. For instance, at 60 °C, the viscosity of the four AAILs ranged between 7.8–4.3 mPa s while that of $[bmim]^+[BF_4]^-$was 30 mPa s. The viscosity of the synthesized AAILs also was less than many other conventional ILs. For instance, conventional $[bmim]^+$ and $[emim]^+$ cation based ILs such as $[bmim]^+[TF_2N]^-$, $[bmim]^+[PF_6]^-$, $[emim]^+[BF_4]^-$, and $[emim]^+[TF_2N]^-$ have viscosity values of 69, 450, 43, 32.6 mPa s respectively at 25 °C.[32–34] Therefore, it can be concluded that the synthesized amino acid anion ionic liquids

have significantly less viscosity compared to several conventional ionic liquids.

The thermal decomposition analysis (TGA) of the synthesized AAILs is shown in Fig. 4(a). The Fig. 4(a) confirms that the AAILs are stable up to 300 °C. The thermal stability or the thermal decomposition pattern of the AAILs reported in the present work is in close correspondence with the AAILs reported in literature with other type of cations.[28,29] Shahrom and Wilfred[28] reported the AAILs based on 4-vinylbenzyltrimethylammonium ([VBTMA]) cation and amino acid (AA) anions such as glycinate, alanate and prolinate. The [VBTMA][AA] AAILs showed 80% decomposition at 300 °C.[28] The pattern of decomposition of AAILs of present work also is similar to the [VBTMA] based AAILs reported by Shahrom and Wilfred.[28] Brzeczek-Szafran *et al.*[29] have reported AAILs based on carbohydrate cation. The carbohydrate cation based AAILs as reported by Brzeczek-Szafran *et al.* also showed 80% decomposition at 300 °C.[29] The thermal stability of the AAILs could be attributed to the presence of functional groups such as carboxylate ($-COO^-$) and amine ($-NH_2$) present in amino acid anion. The amino acid anion, due to the presence of carboxylate and amine group, tend to form hydrogen bond within anion and with acidic hydrogen present in the imidazolium cation. Because of this, the degradation will happen gradually as the hydrogen bonds need to be broken first for the decomposition to progress.

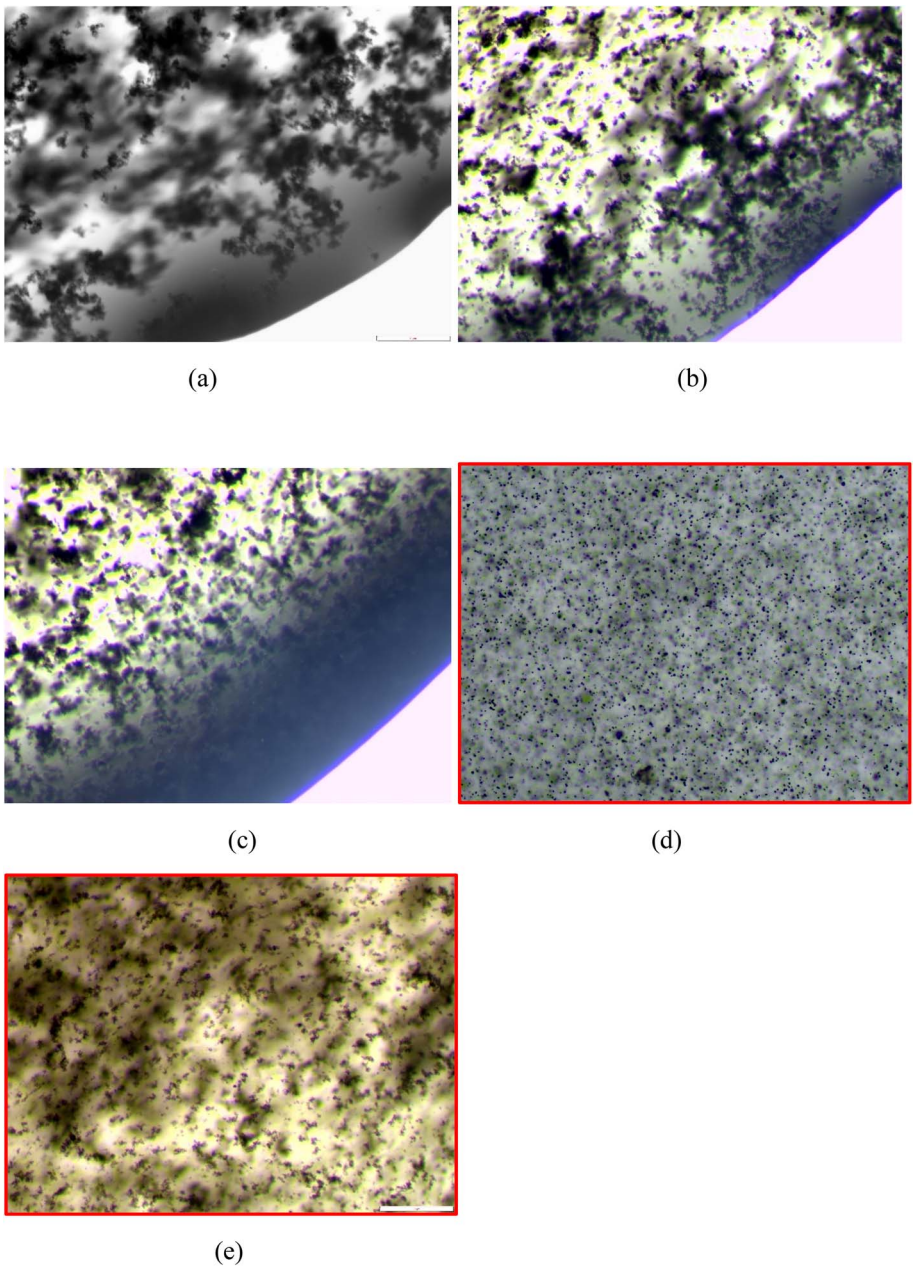

Fig. 5 Effect of surfactant on MWCNT dispersion: (a) [bmim][BF_4] + 0.05% w/w MWCNT (b) [bmim][BF_4] + 0.05% w/w MWCNT + Licithin (c) [bmim][BF_4] + 0.05% w/w MWCNT + SDS (d) [bmim][BF_4] + 0.05% w/w MWCNT + Tween 80 (e) [bmim][BF_4] + 0.05% w/w MWCNT + CTAB (better dispersion images highlighted in red).

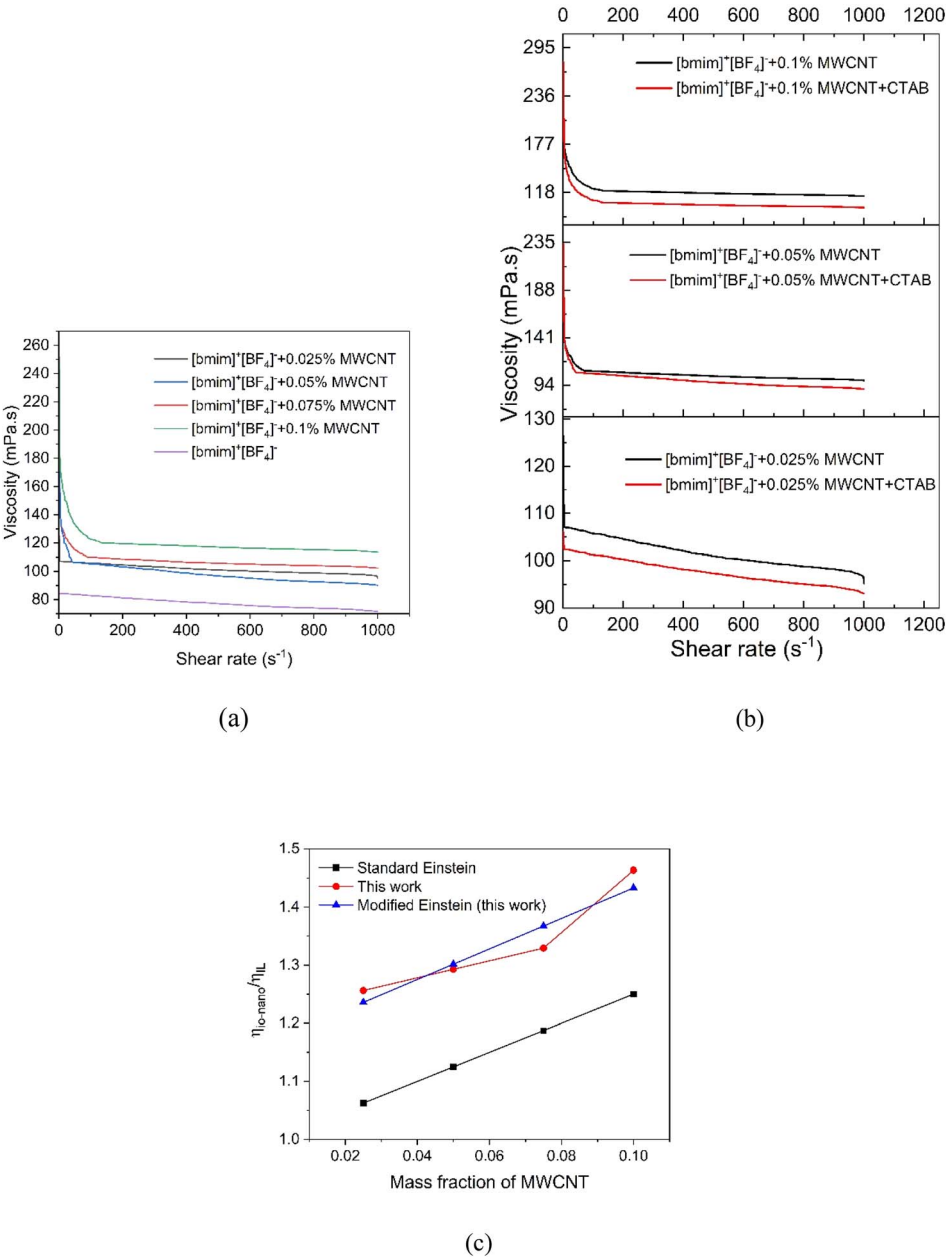

Fig. 6 Viscosity of $[bmim]^+[BF_4]^-$ based Io-Nanofluids (a) effect of MWCNT concentration (b) effect of surfactant CTAB (c) viscosity enhancement with MWCNT concentration.

The DSC analysis in the temperature range of −80 °C to 310 °C for the four AAILs is presented in Fig. 4(b) and (c). Fig. 4(b) (heat flow *vs.* temperature) shows that the glass transition temperature was not observed for the synthesized AAILs in the analysed temperature range. This indicates that the glass transition temperature for the studied AAILs is definitely less than −80 °C. Further, the DSC plots of all the AAILs showed a broad endotherm between 5–170 °C having a peak at around 96–108 °C corresponding to gradual phase transition due to melting. The enthalpy of fusion of $[bmim]^+[Gly]^-$, $[bmim]^+[Arg]^-$, $[emim]^+[Gly]^-$, and $[emim]^+[Arg]^-$ as calculated from the DSC curves were 313.09, 418.37, 341.51, 506.98 J g^{-1} respectively. The enthalpy of fusion of AAILs synthesized in present work was observed to be significantly less than that of several conventional ILs. For instance, the enthalpy of fusion of $[bmim]^+[TF_2N]^-$, and $[bmim]^+[BF_4]^-$ are 28.7 kJ mol^{-1} and 37.2 kJ mol^{-1} respectively.[35,36] Furthermore, it can be observed that the enthalpy of fusion of Glycinate anion AAIL is lower than the Argininate anion AAIL. This can be attributed to the presence of more amine groups in Argininate anion which results in the formation of more inter-ionic hydrogen bond network. Therefore, more energy is required to break the inter-ionic hydrogen bonds. Another endotherm between 220–270 °C having a peak at 250 °C corresponds to the decomposition of the IL. The gradual melting of the AAILs could be attributed to the presence of hydrogen bond network present between the

amino acid anion and cation and between the amino acid anions because of functional groups such as carboxylate ($-COO^-$) and amine ($-NH_2$). Fig. 4(c) shows that the specific heat capacity of the AAILs follows the order of $[emim]^+[Arg]^-$ (14.15 J g^{-1} °C^{-1}) > $[bmim]^+[Arg]^-$ (11.03 J g^{-1} °C^{-1}) > $[emim]^+[Gly]^-$ (7.92 J g^{-1} °C^{-1}) > $[bmim]^+[Gly]^-$ (6.30 J g^{-1} °C^{-1}). Higher specific heat capacity of a heat transfer fluid denotes that the fluid can absorb, store and transfer more energy per unit mass per unit temperature and also can maintain stable temperature with less fluctuations which finally results in better heat transfer properties. Therefore, the studied AAILs could be ranked in the order of $[emim]^+[Arg]^-$ > $[bmim]^+[Arg]^-$ > $[emim]^+[Gly]^-$ > $[bmim]^+[Gly]^-$ in terms of both viscosity and heat capacity. Furthermore, the specific heat capacity of AAILs of present work observed to be substantially higher than conventional ILs. For instance, the specific heat capacity of $[emim]^+[BF_4]^-$ and $[bmim]^+[TF_2N]^-$ are 1.566 J g^{-1} °C^{-1}, 1.35 J g^{-1} °C^{-1} only,[34,35] while that for the AAILs synthesized in the present work was in the range of 6–14 J g^{-1} °C^{-1} (Fig. 4(c)).

3.3. Characterization of IoNanofluids

3.3.1. Density of IoNanofluids. The density of the INFs synthesized is reported in Tables 2 and 3 respectively. With the addition of MWCNT in low mass fractions (0.025–0.1 wt%), the density of the IoNanofluid slightly increased. This minimal increase in density was due to the very low concentration of MWCNT added. The increase in density of IL after MWCNT addition was observed to be slightly higher in case of AAIL compared to $[bmim]^+[BF_4]^-$. In case of AAIL INFs, the increase in density of AAIL INF with reference to the parent AAIL observed to be affected by the type of cation and anion and their combination. Furthermore, the surfactant did not show any significant effect on the INF density. The density of the INF changed very insignificantly with the addition of surfactant. For instance, the density of ILCNT4 ($[bmim]^+[BF_4]^-$ + 0.1 wt% MWCNT) was 1.223 g cm^{-3} while the density of CTAB added ILCNT8 ($[bmim]^+[BF_4]^-$ + 0.1 wt% MWCNT + CTAB) was 1.221 g cm^{-3} (Table 2). This minimal/insignificant change in density of nanofluid with the addition of surfactant could be because of the fact that the density of the nanofluid depends predominantly on the type of base fluid and the concentration of nanoparticles. The surfactant only aids in reducing the nanoparticle agglomeration and improving the nanofluid stability by reducing the nanoparticle aggregation and sedimentation to improve overall heat transfer efficiency.

3.3.2. Effect of surfactant. Uniform and fine dispersion of nanoparticles in the HTF solution are critical factors to favour enhanced thermal conductivity and heat transfer efficiency of IoNanofluids compared to their pure solvent counterparts. Surfactants are the molecules consisting of hydrophilic head and hydrophobic tail parts. They could essentially prevent the agglomeration of MWCNT nanoparticles by reducing the surface tension between the nanoparticles and the base fluid and by creating electrostatic repulsive forces between the nanoparticles. The surfactant adsorbed on the nanoparticle through hydrophobic tail part would alter the surface charge of the nanoparticles. This creates electrostatic repulsive forces which counteracts the van der Waals attractive forces between the nanoparticles. This ultimately leads to fine dispersion of nanoparticles. This way, the adsorbed surfactant would also modify the nanoparticle–fluid interface which prevents further aggregation. These phenomena therefore promote fine and homogeneous dispersion of nanoparticles in the nanofluid and prevent agglomeration and sedimentation of nanoparticles over time. The effect of nature of surfactants on the nanoparticle size and uniformity of dispersion was studied for $[bmim]^+[BF_4]^-$ IoNanofluid. Various surfactants such as Soy lecithin (amphoteric), Sodium dodecyl sulphate (SDS, anionic), Tween 80 (polysorbate 80, non-ionic) and CTAB (cationic) were evaluated. The surfactants were added to the INF in equal concentration as MWCNT. The effect of surfactant on the nanoparticle agglomerate size and dispersion in the 0.05 wt% MWCNT added $[bmim]^+[BF_4]^-$ against the INF without surfactant were compared in Fig. 5. The details of the amount of surfactant added are shown in Table 2. As per Fig. 5, in terms of enhanced dispersion, the studied surfactants can be ranked in the order of Tween 80 > CTAB > SDS > Licithin. The surfactant Tween 80 showed excellent performance in terms of reducing nanoparticle size and improving uniformity of dispersion. However, with respect to the number of days of colloidal stability, the surfactants can be ranked as CTAB (14 days) > Licithin (11 days) > Tween 80 (8 days) > SDS (6 days). Therefore, although Tween 80 provided better dispersion and finer particles, CTAB showed better performance in terms of colloidal stability.

3.3.3. Viscosity. Viscosity of the $[bmim]^+[BF_4]^-$ + MWCNT IoNanofluid with respect to shear rate (s^{-1}) in a range of 1–1000 s^{-1} at 298 K is plotted in Fig. 6(a). The Fig. 6(a) infers that the pure $[bmim]^+[BF_4]^-$ as well as the INFs at all MWCNT concentrations exhibited Newtonian behaviour. Further, the viscosity increased with increase in concentration of MWCNT from 0.025–0.1 wt%. Also, the viscosity of the INF was observed to decrease with the addition of CTAB surfactant as shown in

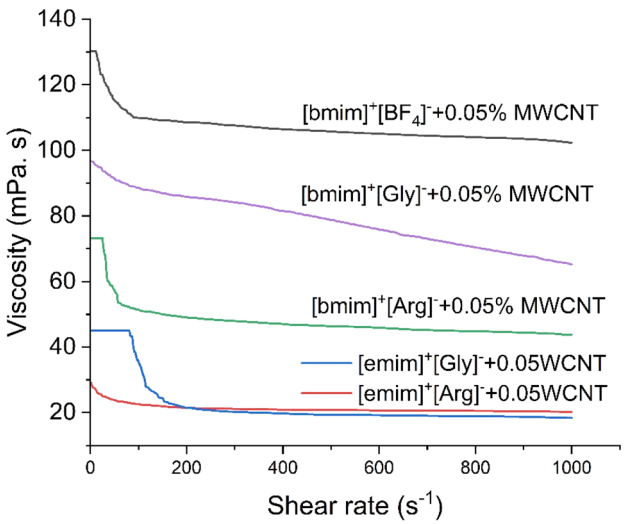

Fig. 7 Shear rate *versus* viscosity comparision for Io-Nanofluid based on AAIL and $[bmim]^+[BF_4]^-$.

Fig. 6(b). The lubrication activity of the surfactant results in reduced viscosity of the INF (Fig. 6(b)). The relative viscosity ratio of $[bmim]^+[BF_4]^-$ IoNanofluid *versus* pure $[bmim]^+[BF_4]^-$ was plotted against the mass fraction of MWCNT. An increase in mass fraction of nanoparticles increased the viscosity. The data was fitted to a standard Einstein model (eqn (1))[35,36] and modified Einstein model (eqn (2)) as per equations below and presented in Fig. 6(c).

$$\frac{\eta_{\text{io-nano}}}{\eta_{\text{IL}}} = 1 + 2.5\varphi \text{ (ref. 37 and 38)} \quad (1)$$

$$\frac{\eta_{\text{io-nano}}}{\eta_{\text{IL}}} = 1.17 + 2.63\varphi \quad (2)$$

The modified Einstein model (eqn (2)) gave a better fit to the experimental data.

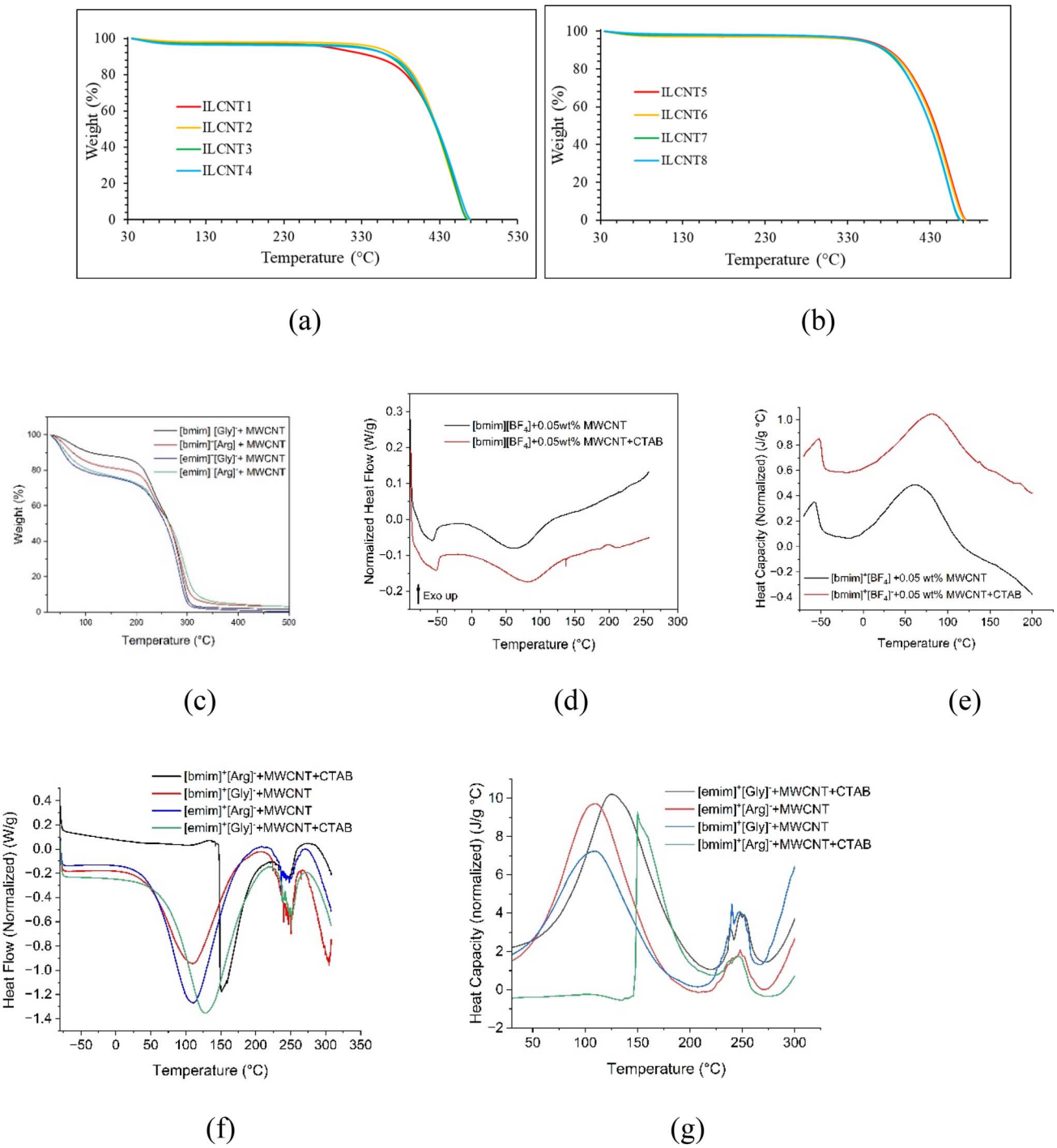

Fig. 8 (a) and (b) TGA of $[bmim]^+[BF_4]^-$ INFs (codes as per Table 2), (c) TGA of AAIL INFs (d) heat flow *vs.* temperature of $[bmim]^+[BF_4]^-$ INFs (e) heat capacity *vs.* temperature of $[bmim]^+[BF_4]^-$ INFs (f) heat flow *vs.* temperature of AAIL INFs (g) heat capacity *vs.* temperature of AAIL INFs.

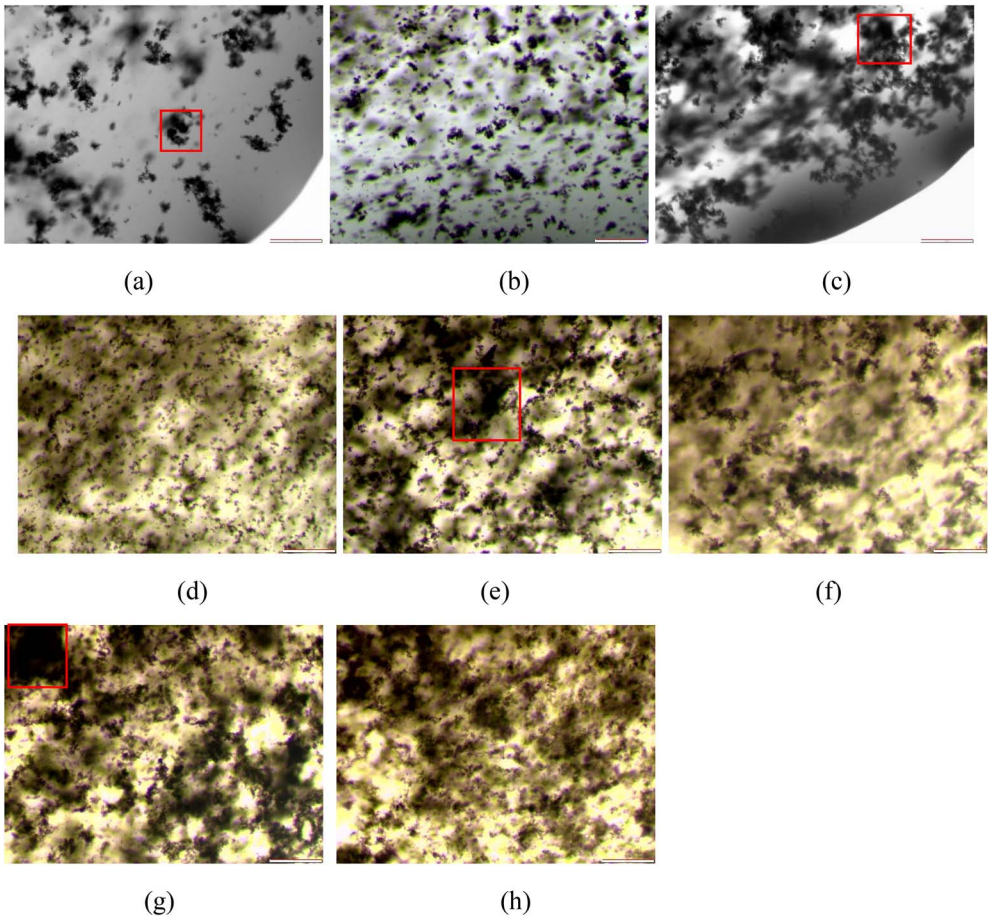

Fig. 9 (a) [bmim][BF_4] + 0.025% w/w MWCNT (b) [bmim][BF_4] + 0.025% w/w MWCNT + CTAB (c) [bmim][BF_4] + 0.05% w/w MWCNT (d) [bmim][BF_4] + 0.05% w/w MWCNT + CTAB(e) [bmim][BF_4] + 0.075% w/w MWCNT (f) [bmim][BF_4] + 0.075% w/w MWCNT + CTAB (g) [bmim][BF_4] + 0.1% w/w MWCNT (h) [bmim][BF_4] + 0.1% w/w MWCNT + CTAB (agglomerations are highlighted in red squares).

As the 0.1 wt% MWCNT showed highest viscosity of INF (Fig. 6) and 0.025 wt% MWCNT would be very less concentration to achieve the targeted heat transfer properties, 0.05 wt% MWCNT was considered for studying the effect of surfactant and for developing the AAIL INFs. The viscosity *versus* shear rate (in the range of 1–1000 s^{-1}) of the INFs based on synthesized AAILs and $[bmim]^+[BF_4]^-$ at 0.05 wt% concentration of MWCNT was compared in Fig. 7. The Fig. 7 confirms that the IoNanofluid based on AAIL showed significantly less viscosity compared to that based on $[bmim]^+[BF_4]^-$ (18 mPa s *vs.* 110 mPa s at 300 K). Fig. 7 also confirms the Newtonian nature of the AAIL IoNanofluids. Among the four AAIL IoNanofluids studied, $[emim]^+[Gly]^-$ and $[emim]^+[Arg]^-$ showed lowest viscosity which can be attributed to the low alkyl chain length of the cation. The lower viscosity of the AAIL INFs suggests that they provide advantages such as less pumping costs, low pressure drop and improved stability by hindering nanoparticle agglomerations, a better heat transfer efficiency by reducing the losses in convective heat transfer by facilitating free movement of nanoparticles. Therefore, the AAIL INFs have potential to be more promising INFs compared to $[bmim]^+[BF_4]^-$ INFs.

3.3.4. TGA and DSC analysis. The TGA analysis of the $[bmim]^+[BF_4]^-$ IoNanofluids having various concentrations of MWCNT is presented in Fig. 8(a). The effect of surfactant CTAB on the $[bmim]^+[BF_4]^-$ IoNanofluids is presented in Fig. 8(b). The codes are as per details in Table 2. All the $[bmim]^+[BF_4]^-$ IoNanofluids showed thermal stability up to 350 °C. It was observed that addition of CTAB has positively improved the thermal stability (Fig. 8(a) and (b)). The TGA analysis of AAIL IoNanofluids is presented in Fig. 8(c). Comparison of Fig. 4(a) and 8(c) infers that the addition of 0.05 wt% MWCNT had positively improved the thermal stability of AAIL IoNanofluids in terms of on-set and progression of decomposition. Fig. 8(d) and (e) presents the DSC analysis of [bmim][BF_4] + 0.05 wt% MWCNT IoNanofluid and the effect of CTAB addition. Fig. 8(d) shows that the $[bmim]^+[BF_4]^-$ INFs show a glass transition temperature at ≈ −54 °C. The onset of melting observed to be 14 °C and the melting is indicated by a broad and small endotherm with peak position at 60 °C with an enthalpy of 17.59 J g^{-1}. The on-set of decomposition (oxidation) at 250 °C is also visible in Fig. 8(d) for $[bmim]^+[BF_4]^-$ Io-Nanofluid. Fig. 8(e) shows the heat capacity *vs.* temperature of $[bmim]^+[BF_4]^-$ INFs. The heat capacity of the $[bmim]^+[BF_4]^-$ with 0.05 wt% MWCNT was 0.4 J

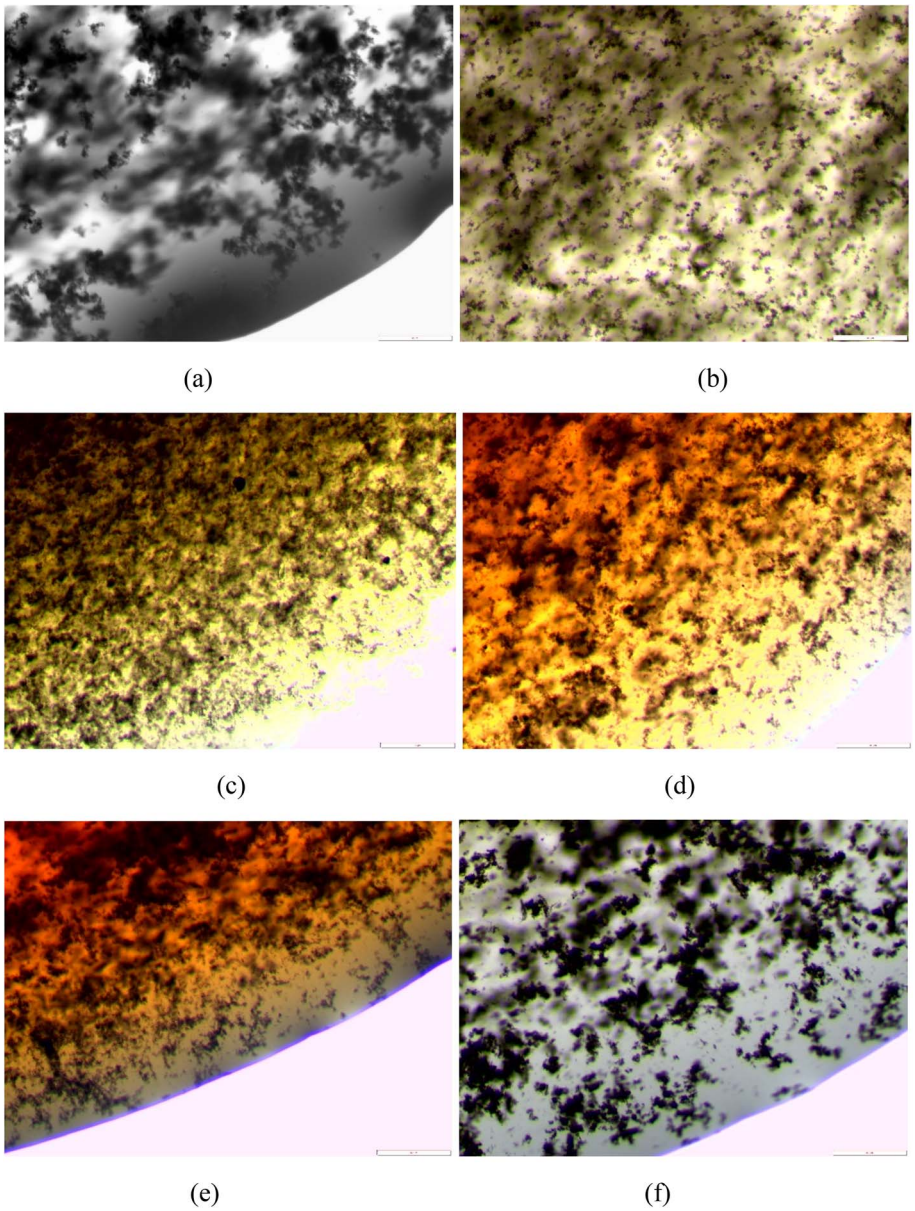

Fig. 10 (a) [bmim][BF_4] + 0.05% w/w MWCNT (b) [bmim][BF_4] + 0.05% w/w MWCNT + CTAB (c) [bmim][Arg] + 0.05% w/w MWCNT (d) [bmim][Arg] + 0.05% w/w MWCNT + CTAB (e) [emim][Gly] + 0.05% w/w MWCNT (f) [bmim][Gly] + 0.05% w/w MWCNT + CTAB.

g^{-1} °C and that of CTAB added $[bmim]^+[BF_4]^-$ with 0.05 wt% MWCNT was around 1.00 J g^{-1} °C. This shows that the heat capacity improved with the addition of surfactant CTAB which can be attributed to the breaking of nanoparticle agglomeration with CTAB addition.[37,38]

Fig. 8(f) and (g) presents the DSC analysis of AAIL IoNanofluids. CTAB was added to $[bmim]^+[Arg]^-$ and $[emim]^+[Gly]^-$. CTAB was not added for $[bmim]^+[Gly]^-$ and $[emim]^+[Arg]^-$. The enthalpy of fusion and peak position of AAIL IoNanofluids was observed to be 210.66 J g^{-1} (151 °C), 388.39 J g^{-1} (130 °C), 336.71 J g^{-1} (111 °C), 441.18 J g^{-1} (112 °C), for $[bmim]^+[Arg]^-$, $[emim]^+[Gly]^-$, $[bmim]^+[Gly]^-$, and $[emim]^+[Arg]^-$respectively. Compared to the pure AAIL, the peak position of the melting endotherm slightly increased and the enthalpy of fusion decreased probably due to the presence of MWCNT and CTAB (Fig. 4(b) *vs.* Fig. 8(f)). The peak position of melting significantly improved for the CTAB added $[bmim]^+[Arg]^-$ and $[emim]^+[Gly]^-$ IoNanofluids. For the other two AAILs, enthalpy of fusion decreased significantly along with a slight increase in peak melting temperature. Comparison of Fig. 8(g) and 4(c) indicates that the addition of MWCNT decreased the specific heat capacity of AAILs due to the heat conductive properties of MWCNT. Fig. 8(d) and (g) clearly indicates that the specific heat capacity of AAIL based IoNanofluids was remarkably higher than that of $[bmim]^+[BF_4]^-$ IoNanofluid. For instance, the heat capacity of CTAB added $[bmim]^+[BF_4]^-$ Io-Nanofluid was 1.00 J g^{-1} °C only, while that for $[emim]^+[Arg]^-$ IoNanofluid was 10.00 J g^{-1} °C (Fig. 8(d) *vs.* 8(g)). This confirms that the AAIL based

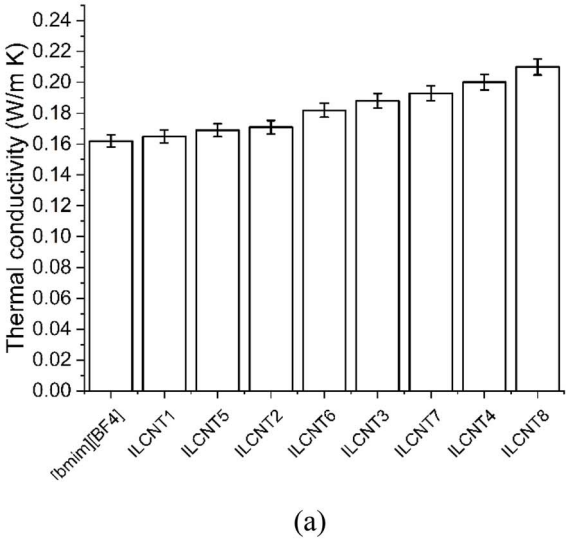

(a)

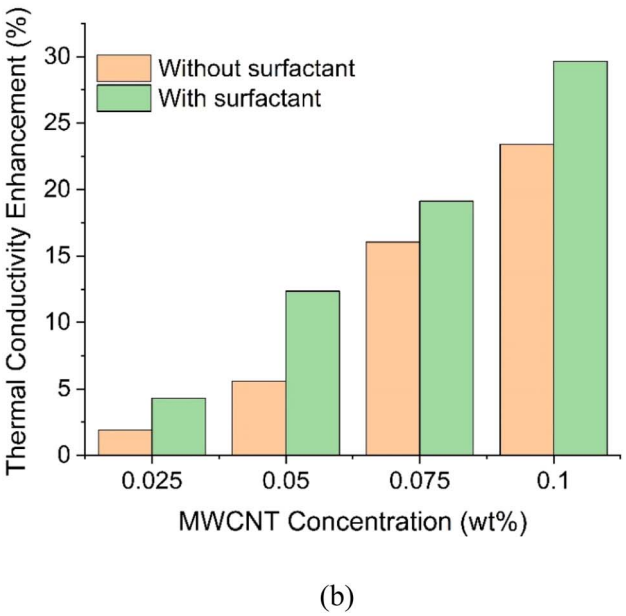

(b)

Fig. 11 (a) Thermal conductivity of $[bmim]^+[BF_4]^-$ based Io-Nanofluid (ILCNT code as per Table 2) (b) thermal conductivity enhancment with respect to pure IL.

IoNanofluids are remarkably suitable as heat transfer fluids compared to conventional IL based INFs. The AAIL INFs can be put in the order of $[emim]^+[Gly]^- \approx [emim]^+[Arg]^- > [bmim]^+[Arg]^- > [bmim]^+[Gly]^-$ in terms of heat capacity. The HTFs such as water and ethylene glycol typically show very less thermal stability. For example, water has a boiling point of 100 °C while ethylene glycol has a boiling point of 193 °C. The specific heat capacity of water is 4.184 J g^{-1} K^{-1} while that of ethylene glycol is 2.4 J g^{-1} K^{-1}.[39] The DSC analysis shows the melting of AAILs at ~99 °C and degradation at ~250 °C. Fundamentally, ionic liquids do not exhibit boiling point but only undergo thermal degradation. This is due to their negligible vapor pressure which makes them degrade before the

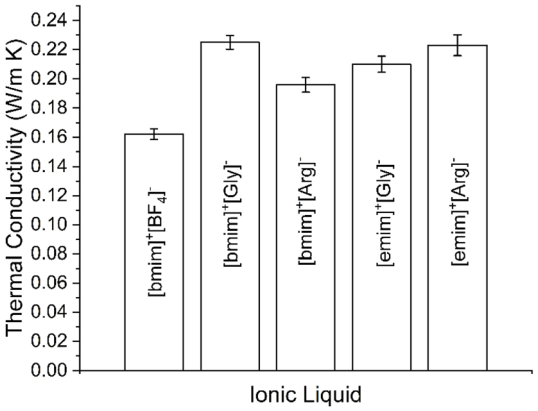

Fig. 12 Thermal conductivity of AAILs in comparision to $[bmim]^+[BF_4]^-$.

temperature reaches atmospheric pressure. Higher specific heat capacity implies the ability of the nanofluid to absorb and store more heat energy per unit temperature raise. This results in enhanced thermal energy storage per unit volume of the HTF which would provide benefit in terms of less volume of HTF required. Further advantages include reduced temperature fluctuations of the fluid and overall enhanced heat transfer.

3.3.5. Nanoparticle dispersion. Fig. 9 displays the microscopic pictures of the $[bmim]^+[BF_4]^-$ IoNanofluid having various concentrations of MWCNT and the effect of CTAB on the MWCNT dispersion. Fig. 9(a), (c), (e) and (g) clearly shows relatively large agglomerations of MWCNT in the IL phase in the absence of surfactant. Fig. 9(b), (d), (f) and (h) display that the addition of CTAB promotes breaking of nanoparticle agglomerations to smaller ones and improves uniform dispersion. Because of this, small and well spread MWCNT nanoparticles can be seen in the microscopic pictures of IoNanofluid in which CTAB was added (Fig. 9(b), (d), (f) and (h)).

Fig. 10 compares the microscopic picture of the dispersion of 0.05 wt% MWCNT nanoparticles in $[bmim]^+[BF_4]^-$ and AAILs and the effect of CTAB surfactant. It can be visibly confirmed from Fig. 10 that the synthesized AAILs were able to favour finer and uniform dispersion of MWCNT nanoparticles even without surfactant CTAB, compared to $[bmim]^+[BF_4]^-$. The fine dispersion of the nanoparticles in the AAILs could be attributed to their low viscosity.

3.3.6. Thermal conductivity. The purpose of synthesizing IoNanofluids from ILs was to enhance the thermal conductivity of the ILs to make them suitable for HTF applications. Since the viscosity increases by the addition of nanoparticles to the ILs, the enhancement in thermal conductivity is a key factor in determining whether the losses incurred by the increase in viscosity are compensated by the gains made by the enhanced thermal conductivity. Thermal conductivity of $[bmim]^+[BF_4]^-$ IoNanofluids at various MWCNT concentrations is compared in Fig. 11. The size of error bar reflects the error in measurement of thermal conductivity as per the instrument measurement accuracy. The effect of surfactant CTAB on thermal conductivity is also compared in Fig. 11. The codes ILCNT1 and ILCNT5

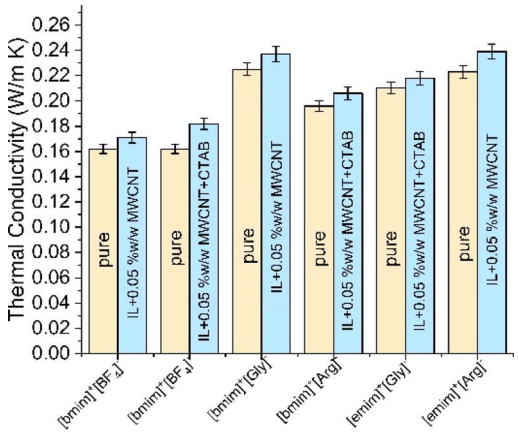

(a)

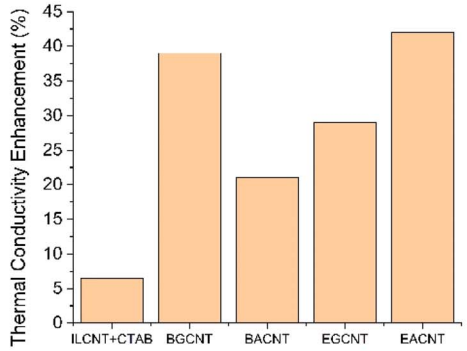

(b)

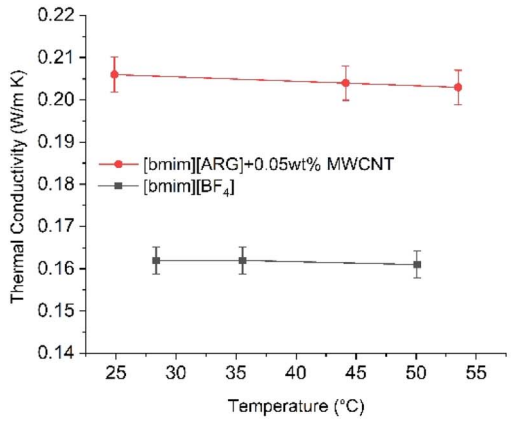

(c)

Fig. 13 (a) Comparison of thermal conductivity of Io-Nanofluids (b) enhancement in thermal conductivity of AAIL Io-Nanofluid with respect to [bmim][BF_4] Io-Nanofluid at 0.05 wt% MWCNT (codes as per Tables 2 and 3) (c) effect of temperature on thermal conductivity.

refers to the IL with MWCNT concentration 0.025 wt% without and with CTAB respectively. Similarly, ILCNT2 and ILCNT6 compares the effect of CTAB at 0.05 wt% of MWCNT; ILCNT3 and ILCNT7 compares the effect of CTAB at 0.075 wt% of MWCNT; ILCNT4 and ILCNT8 compares the effect of CTAB at 0.1 wt% of MWCNT. The Fig. 11(a) evidently confirms that the thermal conductivity of the MWCNT incorporated IoNanofluid was higher than that of pure IL. The enhancement percent in thermal conductivity of IoNanofluid with and without surfactant compared to pure $[bmim]^+[BF_4]^-$ is shown in Fig. 11(b). The thermal conductivity of IoNanofluid observed to increase with increase in MWCNT concentration (Fig. 11(b)). Also, the addition of CTAB surfactant had further increased the thermal conductivity. The increase in thermal conductivity with the addition of surfactant could be attributed to the decrease in nanoparticle agglomeration and increase in dispersion and lubrication of the MWCNT in the IL.

The thermal conductivity of synthesized AAILs was observed to be higher compared to the commercial IL $[bmim]^+[BF_4]^-$ as shown in the Fig. 12. The width of error bar indicates the error in measurement of thermal conductivity and the instrument measurement accuracy. The four pure AAILs showed thermal conductivity enhancement of 21, 30%, 37% and 42% respectively compared to the pure IL $[bmim]^+[BF_4]^-$ (as shown in Fig. 12). The highest thermal conductivity was shown by $[bmim]^+[Gly]^-$ (0.225 *vs.* 0.16 W m^{-1} K^{-1}) and $[emim]^+[Arg]^-$ (0.223 *vs.* 0.16 W m^{-1} K^{-1}). Fundamentally, the ionic liquids exhibit thermal conductivity due to the presence of ions (cations and anions) while being in liquid state which facilitates the heat transfer by transmission of kinetic energy between ions. Among the ionic liquids, the type of cation, anion and cation–anion interactions will further affect the thermal conductivity. Stronger cation–anion interactions, more ionic mobility and low viscosity are important to achieve high thermal conductivities in ionic liquids. The higher thermal conductivity exhibited by AAILs could be attributed to the presence of hydrogen bond interactions between cation and anion and higher mobility of cation and anion of AAILs due to their low viscosity (Fig. 3).

Fig. 13(a) compares the thermal conductivity of pure $[bmim]^+[BF_4]^-$ and AAILs with the corresponding INFs at 0.05 wt% MWCNT concentration and highlights the effect of surfactant CTAB. Further, the enhancement in thermal conductivity of AAIL INFs compared to $[bmim]^+[BF_4]^-$ at 0.05 wt% MWCNT concentration are presented in Fig. 13(b). It is evident from Fig. 13 that the thermal conductivity of all the pure and MWCNT added AAILs was higher than the MWCNT and CTAB added $[bmim]^+[BF_4]^-$. The four AAIL INFs showed thermal conductivity enhancement of 21%, 28%, 39% and 40% respectively compared to the $[bmim]^+[BF_4]^-$ INF. Further, the thermal conductivity of AAIL INF increased by ≈10% with the addition of 0.05 wt% of MWCNT. Also, CTAB does not seem to show any significant effect on thermal conductivity of AAILs. The reason might be the already less viscous AAILs provided good dispersion of MWCNT which is critical for improved thermal conductivity. The factors which drive the thermal conductivity enhancement for a fixed type and concentration of

nanoparticles are (i) thermal conductivity and viscosity of the base fluid, (ii) viscosity of INF after nanoparticle addition (iii) nanoparticle size, (iv) nanoparticle dispersion and homogeneity. Fig. 13(c) compares the effect of temperature on the thermal conductivity of the pure IL $[bmim]^+[BF_4]^-$ and the INF [bmim][ARG] + 0.05 wt% MWCNT in the temperature range of 25–50 °C. Fig. 13(c) shows that, in the studied temperature range, for both the INFs, the thermal conductivity only slightly reduced from 25/28 °C to 50 °C/53 °C. With increase in temperature, the thermal conductivity of liquids generally decreases due to increased distance between the molecules which reduces the effective collisions required for heat transfer. Similarly, the thermal conductivity of individual MWCNT particle also decreases at higher temperatures due to increased phonon scattering which results in loss of phonon energy and disrupted coherent flow of heat. Sometimes, due to the morphological factors, the MWCNTS could show an increase in thermal conductivity and then a reduction. However, with respect to nanofluids, the increase in temperature may cause Brownian motion of nanoparticles which could increase the collisions between nanoparticles finally resulting in increased thermal conductivity. Therefore, because of the combined effect, the overall thermal conductivity of the INFs got reduced only slightly with an increase in temperature within the low temperature range considered in the present study. The decrease in thermal conductivity of the INFs at very high temperatures would restrict the applicability of the INFs in terms of operating temperature range. In the present study, we have evaluated the thermal conductivity up to 50 °C only due to the limitations of the instrument. To evaluate the heat transfer

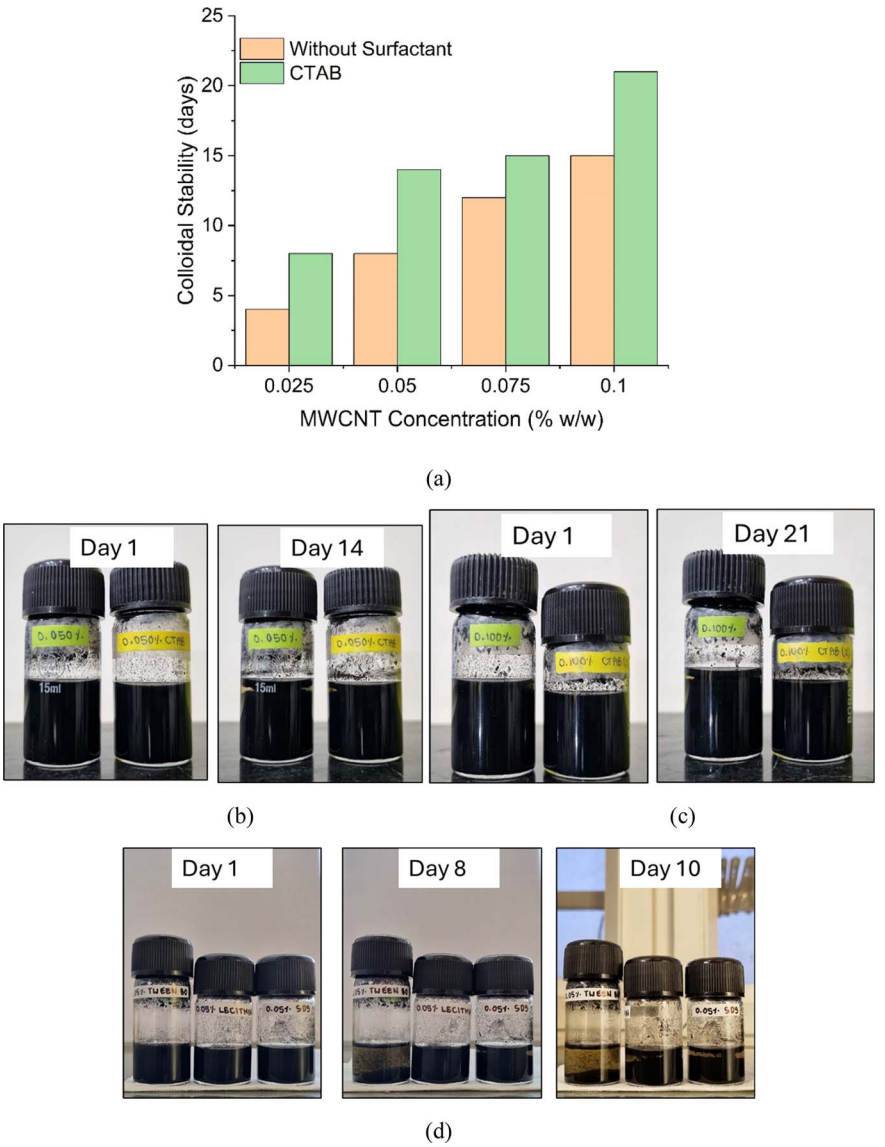

Fig. 14 (a) Effect of MWCNT concentration and CTAB addition on the colloidal stability of $[bmim]^+[BF_4]^-$ Io-Nanofluids. (b) Colloidal stability of Io-Nanofluid with 0.05 wt% MWCNT (c) colloidal stability of Io-Nanofluid with 0.1 wt% MWCNT (d) colloidal stability of Io-Nanofluid with 0.05 wt% MWCNT with Tween 80, Licithin and SDS.

efficiency of INFs for higher temperatures, the thermal conductivity needs to be measured for the required temperature range.

3.3.7. Colloidal stability. Colloidal stability is another key performance indicator of the IoNanofluids. The non-uniform dispersion of nanoparticles (lack of homogeneity) would cause HTFs losing the heat transfer efficiency. For instance, localized regions with higher concentration of nanoparticles results in more heat transfer in those regions whereas the regions of lower nanoparticle concentrations would show less heat transfer. This may lead to reduction in overall heat transfer. Therefore, the colloidal stability of the INFs based on $[bmim]^+[BF_4]^-$ and AAILs was studied as per the procedure mentioned in Section 2.4.8.

Fig. 14 shows the effect of MWCNT concentration and CTAB addition on the colloidal stability in terms of number of days for $[bmim]^+[BF_4]^-$ INFs. The IoNanofluid samples were stocked in glass vials and kept undisturbed. The vials were then observed every day for any visible settling of MWCNT particles. It was observed that the addition of CTAB has considerably increased the shelf life of MWCNT colloidal dispersion of $[bmim]^+[BF_4]^-$ (Fig. 14(a)–(c)). For instance, the nanoparticle suspension of INF having 0.05 wt% of MWCNT was stable for 8 days only. However, addition of CTAB has increased the nanoparticle suspension stability to 14 days. Furthermore, the colloidal dispersion stability (number of days) increased with increase in MWCNT concentration (Fig. 14(a)–(c)). For representational purpose, the pictures of the vials corresponding to 0.05 wt% and 0.1 wt% MWCNT are presented in Fig. 14(b) and (c) respectively. For comparison purpose, the colloidal stability of the $[bmim]^+[BF_4]^-$ INFs having 0.05 wt% MWCNT with other surfactants such as Tween 80, lecithin and SDS is shown in Fig. 14(d). It was observed that the INFs having Tween 80, lecithin and SDS were stable for 8, 10 and 8 days respectively which is considerably less compared to the CTAB based INF.

Fig. 15 compares the colloidal dispersion stability of IoNanofluids of AAIL and $[bmim]^+[BF_4]^-$ at MWCNT concentration of 0.05 wt%. It can be evidently confirmed from Fig. 15 that the AAIL + MWCNT IoNanofluids showed substantially higher colloidal stability (30 days) compared to the $[bmim]^+[BF_4]^-$ + MWCNT (7 days) and $[bmim]^+[BF_4]^-$ + MWCNT + CTAB (14 days). The improved colloidal stability of AAIL INFs could be due to (i) the low viscosity of the AAIL, (ii) interaction between AAIL and MWCNT, (iii) the collective effect of the surfactant and polarity of the AAIL in altering the surface charges of the nanoparticles which created required electrostatic repulsive forces between nanoparticles to form relatively finer and homogeneous dispersion of nanoparticles in the AAIL INFs. The surfactant CTAB compatibility with AAIL and MWCNT might have further hampered the agglomeration and sedimentation of the nanoparticles.

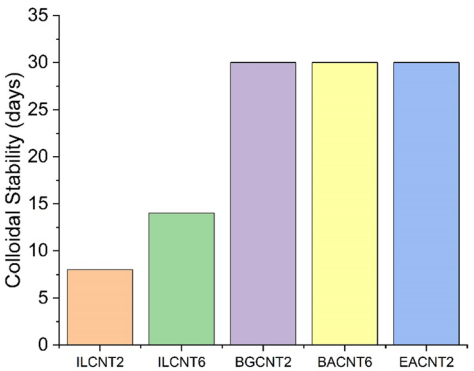

(a)

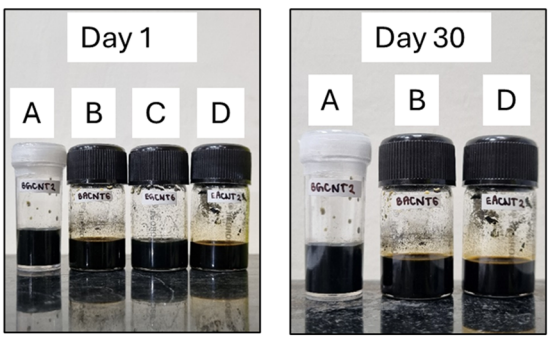

(b)

Fig. 15 (a) Colloidal stability comparison of $[bmim]^+[BF_4]^-$ INF and AAIL INF having 0.05 wt% of MWCNT (b) colloidal stability of AAIL INFs having 0.05 wt% of MWCNT.

4. Conclusions

IoNanofluids of $[bmim]^+[BF_4]^-$ were prepared by adding various concentrations of MWCNT. Effect of MWCNT concentration and surfactant on the properties of $[bmim]^+[BF_4]^-$ with respect to HTF applications was studied. It was observed that, the viscosity of the IoNanofluid increased with the increase in concentration of MWCNT. However, an increase in thermal conductivity was observed with increase in MWCNT concentration. Among the four surfactants tested, Tween 80 showed finer and uniform nanoparticle dispersion but did not give much advantage in terms of colloidal stability. CTAB was observed to be a better surfactant in terms of nanoparticle dispersion, colloidal stability and thermal conductivity improvement. The synthesized AAILs showed significantly less viscosity (18–8 mPa s at 298 K) compared to several conventional ILs. The AAIL + 0.05 wt% MWCNT IoNanofluids showed ~42% higher thermal conductivity than $[bmim]^+[BF_4]^-$ + 0.05 wt% MWCNT (0.24 W m^{-1} K^{-1} *vs.* 0.18 W m^{-1} K^{-1} at ~300 K) and very less viscosity (20 mPa s *vs.* 110 mPa s at ~300 K). The AAIL + MWCNT IoNanofluids showed fine and uniform dispersion of MWCNT and substantially higher colloidal stability (30 days) compared to the $[bmim]^+[BF_4]^-$ + MWCNT (7 days) and $[bmim]^+[BF_4]^-$ + MWCNT + CTAB (14 days). The AAIL-INFs showed significantly higher specific heat capacity compared to $[bmim]^+[BF_4]^-$ INF (1.00 J g^{-1} °C *vs.* 10.00 J g^{-1} °C). Therefore, the present study introduces the AAIL based INFs which showed superior properties compared to conventional IL based INFs that are required for potential heat transfer fluids.

Data availability

No new data were generated or analyzed in this study, and therefore, a data availability statement is not applicable. Any data supporting this article have been included as part of the ESI.†

Author contributions

Conceptualization, methodology, supervision, writing – original draft, Y. S. S. (Yamini Sudha Sistla); investigation, data curation, validation, A. C. (Anshu Chandra), M. A. A. (Mir Atiq Ahmed), D. V. S. V. (Durga Vijay Shankar Vasireddy); formal analysis, investigation, resources, N. J. (Nancy Jaglan), N. K. D. (Nipu Kumar Das), T. B. (Tamal Banerjee), V. S. S. (Venkata Subbarayudu Sistla).

Conflicts of interest

There are no conflicts to declare.

Acknowledgements

The authors would like to acknowledge Prof. Bimlesh Lochab, Department of Chemistry, Shiv Nadar Institution of Eminence, for providing multiwalled carbon nanotubes. The authors would like to acknowledge Prof. Sajal Ghosh, Department of Physics, Shiv Nadar Institution of Eminence, for providing viscometer facility. The authors would like to acknowledge Dr Ashish Kumar Thokchom, Department of Chemical Engineering, Shiv Nadar Institution of Eminence, for providing optical microscope facility.

References

1 A. Lenert, Y. Nam and E. N. Wang, Heat Transfer Fluids, *Annu. Rev. Heat Transf.*, 2012, **15**, 93–129, DOI: 10.1615/AnnualRevHeatTransfer.2012004122.

2 D. Dewanjee and B. Kundu, A review of applications of green nanofluids for performance improvement of solar collectors, *Renewable Energy*, 2025, **240**, 122182, DOI: 10.1016/j.renene.2024.122182.

3 B. Heidarshenas, Y. Yuan and A. S. El-Shafay, Advancements in 2D nanomaterial-enhanced nanofluids: Stability, thermophysical properties, and industrial applications, *Powder Technol.*, 2025, **454**, 120687, DOI: 10.1016/j.powtec.2025.120687.

4 E. Mansi, I. Balog, G. Caputo, N. Corsaro, I. D. Sarcina, G. Tiranti, F. Filippi, F. Panza, N. Ratto, S. Sau, A. Simonetti, A. Spadoni, A. C. Tizzoni, A. Cemmi and M. Ciotti, Bluesil FLD 550 HT Silicone Oil as Heat Transfer Fluid for Power Plant Applications: Thermal Stability Properties, *Appl. Sci.*, 2025, **15**, 2340, DOI: 10.3390/app15052340.

5 M. Kalbarczyk, S. Skupinski and M. Kosmulski, Heat Transfer Fluids Based on Amino-Functionalized Silica Dispersed in 1,2-Propylene Glycol and in 50-50 Aqueous 1,2-Propylene Glycol, *Colloids Interfaces*, 2024, **8**, 43, DOI: 10.3390/colloids8040043.

6 R. Si, D. Jing, F. Liu, D. Kong, X. Liu and J. Lu, The development and application of Silicone-based heat transfer fluids, *J. Phys.: Conf. Ser.*, 2023, **2539**, 012083, DOI: 10.1088/1742-6596/2539/1/012083.

7 E. A. Chernikova, L. M. Glukhov, V. G. Krasovskiy, L. M. Kustov, M. G. Vorobyeva and A. A. Koroteev, Ionic liquids as heat transfer fluids: comparison with known systems, possible applications, advantages and disadvantages, *Russ. Chem. Rev.*, 2015, **84**(8), 875–890, DOI: 10.1070/RCR4510.

8 S. U. S. Choi and J. A. Eastman, *Enhancing thermal conductivity of fluids with nanoparticles, developments and applications of non-Newtonian flows*, Report No. ANL/MSD/CP-84938; CONF-951135-29, Argonne National Lab (ANL), Argonne, IL, 1995.

9 E. C. Okonkwo, I. Wole-Osho, I. W. Almanassra, Y. M. Abdullatif and T. Al-Ansari, An updated review of nanofluids in various heat transfer devices, *J. Therm. Anal. Calorim.*, 2021, **145**, 2817–2872, DOI: 10.1007/s10973-020-09760-2.

10 D. Wen, G. Lin, S. Vafaei and K. Zhang, Review of nanofluids for heat transfer applications, *Particuology*, 2009, **7**, 141–150, DOI: 10.1016/j.partic.2009.01.007.

11 K. Jafari, M. H. Fatemi and P. Estellé, Deep eutectic solvents (DESs): A short overview of the thermophysical properties and current use as base fluid for heat transfer nanofluids, *J. Mol. Liq.*, 2021, **321**, 114752, DOI: 10.1016/j.molliq.2020.114752.

12 Y. C. Yan, W. R. M. Khalid, K. Shahbaz, T. C. S. M. Gupta and N. Mase, Potential application of deep eutectic solvents in heat transfer application, *J. Eng. Sci. Technol.*, 2017, **2016**, 1–14.

13 P. Dehury, A. K. Upadhyay and T. Banerjee, Evaluation and conceptual design of triphenylphosphonium bromide-based deep eutectic solvent as novel thermal nanofluid for concentrated solar power, *Bull. Mater. Sci.*, 2019, **42**, 262, DOI: 10.1007/s12034-019-1946-6.

14 G. Kaur, H. Kumar and M. Singla, Diverse applications of ionic liquids: A comprehensive review, *J. Mol. Liq.*, 2022, **351**, 118556, DOI: 10.1016/j.molliq.2022.118556.

15 A. A. Minea and S. M. S. Murshed, Ionic Liquids-Based Nanocolloids—A Review of Progress and Prospects in Convective Heat Transfer Applications, *Nanomaterials*, 2021, **11**, 1039, DOI: 10.3390/nano11041039.

16 T. C. Paul, A. Tikadar, R. Mahamud, A. S. Salman, A. K. M. M. Morshed and J. A. Khan, A Critical Review on the Development of Ionic Liquids-Based Nanofluids as Heat Transfer Fluids for Solar Thermal Energy, *Processes*, 2021, **9**, 858, DOI: 10.3390/pr9050858.

17 I. Moulefera, A. R. Pastor, M. G. Fuster, J. J. Delgado-Marín, M. G. Montalbán, I. Rodríguez-Pastor, A. López-Pérez, I. Martin-Gullon, A. P. Ramallo-González, M. Alarcón and G. Víllora, Novel application for graphene oxide-based ionanofluids in flat plate solar thermal collectors, *Sci. Rep.*, 2024, **14**, 17610, DOI: 10.1038/s41598-024-67874-1.

18 M. A. Rahman, S. M. M. Hasnain, S. Pandey, A. Tapalova, N. Akylbekov and R. Zairov, Review on Nanofluids: Preparation, Properties, Stability, and Thermal Performance Augmentation in Heat Transfer Applications, *ACS Omega*, 2024, **9**, 32328–32349, DOI: **10.1021/acsomega.4c03279**.

19 S. Wcislik, Efficient Stabilization of Mono and Hybrid Nanofluids, *Energies*, 2020, **13**, 3793, DOI: **10.3390/en13153793**.

20 K. Oster, C. Hardacre, J. Jacquemin, A. P. C. Ribeiro and A. Elsinawi, Ionic liquid-based nanofluids (ionanofluids) for thermal applications: an experimental thermophysical characterization, *Pure Appl. Chem.*, 2019, **91**(8), 1309–1340, DOI: **10.1515/pac-2018-1114**.

21 B. Jozwiak, G. Dzido, E. Zorbski, A. Kolanowska, R. Jedrysiak, J. Dziadosz, M. Libera, S. Boncel and M. Dzida, Remarkable Thermal Conductivity Enhancement in Carbon-Based Ionanofluids: Effect of Nanoparticle Morphology, *ACS Appl. Mater. Interfaces*, 2020, **12**, 38113–38123, DOI: **10.1021/acsami.0c09752**.

22 C. A. Nieto de Castro, A. Lamas, X. Paredes, F. J. V. Santos, M. J. V. Lourenco and T. A. Graber, Possible New Heat Transfer Fluid: The IoNanofluid of 1-Ethyl-3-methylimidazolium Dicyanamide + Nano-Titanium Oxide-Studying Its Thermal Conductivity and Viscosity, *J. Chem. Eng. Data*, 2024, **69**, 2227–2235, DOI: **10.1021/acs.jced.4c00167**.

23 J. M. P. Franca, M. J. V. Lourenço, S. M. S. Murshed, A. A. H. Pádua and C. A. Nieto de Castro, Thermal Conductivity of Ionic Liquids and IoNanofluids and their Feasibility as Heat Transfer Fluids, *Ind. Eng. Chem. Res.*, 2018, **57**(18), 6516–6529, DOI: **10.1021/acs.iecr.7b04770**.

24 F.-F. Zhang, F.-F. Zheng, X.-H. Wu, Y.-L. Yin and G. Chen, Variations of thermophysical properties and heat transfer performance of nanoparticle-enhanced ionic liquids, *R. Soc. Open Sci.*, 2018, **6**, 182040, DOI: **10.1098/rsos.182040**.

25 A. Stoppa, O. Zech, W. Kunz and R. Buchner, The Conductivity of Imidazolium-Based Ionic Liquids from (-35 to 195) °C. A. Variation of Cation's Alkyl Chain, *J. Chem. Eng. Data*, 2010, **55**, 1768–1773, DOI: **10.1021/je900789j**.

26 K. Liang, H. Yao, J. Qiao, S. Gao, M. Zong, F. Liu, Q. Yang, L. Liang and D. Fang, Thermodynamic Evaluation of Novel 1,2,4-Triazolium Alanine Ionic Liquids as Sustainable Heat-Transfer Media, *Molecules*, 2024, **29**, 5227, DOI: **10.3390/molecules29225227**.

27 Y. S. Sistla and A. Khanna, CO_2 absorption studies in amino acid-anion based ionic liquids, *Chem. Eng. J.*, 2015, **273**, 268–276, DOI: **10.1016/j.cej.2014.09.043**.

28 M. Shahrom and C. D. Wilfred, Synthesis and Thermal Properties of Amino Acids Ionic Liquids (AAILS), *J. Appl. Sci.*, 2014, **14**, 1067–1072, DOI: **10.3923/jas.2014.1067.1072**.

29 A. Brzeczek-Szafran, P. Wiecek, M. Guzik and A. Chrobok, Combining amino acids and carbohydrates into readily biodegradable, task specific ionic liquids, *RSC Adv.*, 2020, **10**, 18355–18359, DOI: **10.1039/D0RA03664A**.

30 K. J. Hughes, K. A. Iyer, R. E. Bird, J. Ivanov, S. Banerjee, G. Georges and Q. A. Zhou, Review of Carbon Nanotube Research and Development: Materials and Emerging Applications, *ACS Appl. Nano Mater.*, 2024, **7**, 18695–18713, DOI: **10.1021/acsanm.4c02721**.

31 M. Kanakubo and K. R. Harris, Density of 1-Butyl-3-methylimidazolium Bis(trifluoromethanesulfonyl)amide and 1-Hexyl-3-methylimidazolium Bis(trifluoromethanesulfonyl)amide over an Extended Pressure Range up to 250 MPa, *J. Chem. Eng. Data*, 2015, **60**(5), 1408–1418, DOI: **10.1021/je501118w**.

32 J. Li, H. Zhu, C. Peng and H. Liu, Densities and viscosities for ionic liquids [BMIM][BF_4] and [BMIM][Cl] and their binary mixtures at various temperatures and atmospheric pressure, *Chin. J. Chem. Eng.*, 2019, **27**(12), 2994–2999, DOI: **10.1016/j.cjche.2019.04.016**.

33 K. R. Harris, M. Kanakubo and L. A. Woolf, Temperature and Pressure Dependence of the Viscosity of the Ionic Liquids 1-Hexyl-3-methylimidazolium Hexafluorophosphate and 1-Butyl-3-methylimidazolium Bis(trifluoromethylsulfonyl) imide, *J. Chem. Eng. Data*, 2007, **52**(3), 1080–1085, DOI: **10.1021/je700032n**.

34 Y. Qiao, F. Yan, S. Xia, S. Yin and P. Ma, Densities and Viscosities of [Bmim][PF_6] and Binary Systems [Bmim][PF_6] + Ethanol, [Bmim][PF_6] + Benzene at Several Temperatures and Pressures: Determined by the Falling-Ball Method, *J. Chem. Eng. Data*, 2011, **56**(5), 2379–2385, DOI: **10.1021/je1012444**.

35 R. Hamidova, I. Kul, J. Safarov, A. Shahverdiyev and E. Hassel, Thermophysical Properties Of 1-Butyl-3-Methylimidazolium Bis(Trifluoromethylsulfonyl)Imide At High Temperatures And Pressures, *Braz. J. Chem. Eng.*, 2015, **32**(1), 303–316, DOI: **10.1590/0104-6632.20150321s00003120**.

36 H. M. Hasen and B. A. Abdulmajeed, Theoretical investigation of the density and the heat capacity of [EMIM][BF_4] and its MWCNTs ionanofluids: Effect of temperature and MWCNTs concentration, *J. Phys.: Conf. Ser.*, 2021, **2114**, 012036, DOI: **10.1088/1742-6596/2114/1/012036**.

37 Y. O. Solyaev, S. A. Lurie and N. A. Semenov, Generalized Einstein's and Brinkman's solutions for the effective viscosity of nanofluids, *J. Appl. Phys.*, 2020, **128**, 035102, DOI: **10.1063/5.0014288**.

38 D. P. Soman, S. Karthika, P. Kalaichelvi and T. K. Radhakrishnan, Impact of viscosity of nanofluid and ionic liquid on heat transfer, *J. Mol. Liq.*, 2019, **291**, 111349, DOI: **10.1016/j.molliq.2019.111349**.

39 C. Selvam, D. Mohan Lal and S. Harish, Thermal conductivity and specific heat capacity of water–ethylene glycol mixture-based nanofluids with graphene nanoplatelets, *J. Therm. Anal. Calorim.*, 2017, **129**(2), 947–955, DOI: **10.1007/s10973-017-6276-6**.